UNIVERSITY OF CAMBRIDGE
Department of Engineering

JBA consulting

Simulations of Rainfall-Runoff Processes and the Effectiveness of Natural Flood Management

Author Name: Catriona Wallace

Supervisor: Dr. Dongfang Liang

Date: 27th May 2019

I hereby declare that, except where specifically indicated, the work submitted herein is my own original work.

Signed ________________________________ *date* ______________________________

Simulations of Rainfall-Runoff Processes and the Effectiveness of Natural Flood Management Schemes

Catriona Wallace, Emmanuel College

Technical Abstract

This study set out to increase the understanding of rewilding and provide information on how it should be used to decrease the risk of surface water flooding most effectively. This is particularly important due to the rising flood risk, increased expenditure to cover the damages and policy pushes towards increasing resilience using catchment scale NFM measures. Within rewilding land management practices and specifically the natural regeneration of trees and scrubs have been focussed upon. The key aims of this project were to:

- Validate flood modelling software including MacTVD and JFlow against laboratory data and theory.
- Understand the limitations of the software.
- Understand the effectiveness of different rewilding patterns in order to help plan and design for optimal land use.

Literature was reviewed to understand the effects of rewilding and how they could be modelled as well as how these effects have been studied before. It was decided that two 2D hydraulic models (MacTVD and JFlow) would be used in this study. The mathematical basis and numerical method of each model was discussed and the potential advantages and limitations of each were proposed.

MacTVD was then used to replicate data previously collected in the laboratory. Unfortunately JFlow was unable to do this due to the small scale of the experimental catchment. This enabled an understanding of how the outputted hydrographs were produced and the importance of accuracy in the simulation of water velocities. The theory of hydrographs was then investigating to enable dimensionless equations to be proposed. These equations could then be used to compare hydrographs with varying Manning roughness values, rainfall intensities, slope angles and areas.

As JFlow could not be used to replicate the laboratory data, instead the outputted hydrographs were compared to theoretical cases. The roughness, slope angle and rainfall intensity were varied around realistic values to obtain an understanding of the models limitations. It was found that JFlow struggled to accurately simulate very low rainfall intensities, high slope angles and low friction values. Reasons for this were linked back to the mathematical assumptions and numerical methods of the model. The limitations of MacTVD were also investigated and it was found that the model was significantly worse than JFlow at low rainfall levels. This was

improved by increasing the precision of each of the variables.

A baseline case with no rewilding was then created for which all rewilding patterns could be compared to. While creating this baseline, the limitations of the models were considered while trying to maintain realistic parameter values where possible. The baseline case consisted of a V-shaped catchment of size 2.5 km by 2 km, Manning roughness of 0.035 s/m$^{1/3}$, slope angle of 0.05 and rainfall intensity of 100 mm/hr.

The effects of percentage area coverage, location and fragmentation of rewilding were investigated. It was found that increasing the percentage area of coverage (while maintaining a constant location of the rewilded band at the mid-slope), led to a linear increase in the t_{50} time delay compared to the baseline. This is due to the increased roughness of the rewilding slowing the water velocity (subsequently increasing the water depth locally). When rewilding the upper and mid-slopes, a linear increase in t_{50} time delay was also found as the distance from the upper edge of the catchment was increased if the percentage coverage was constant. This allowed an equation to be proposed. However, when the down-slope area close to the channel was rewilded a significant increase in t_{50} was noted. It could also be seen that the maximum water depth was also significantly increased (the upper and mid-slopes had no effect on maximum water depth compared to the baseline case). This interaction between the floodplain and channel would best be studied by a coupled 1D/2D model as 2D models are not designed to simulate channel flow. When studying the effects of fragmentation it was found that splitting the rewilding band had no effect.

Finally, a comparison of the results collected was made to previous studies. The effects of percentage area coverage and fragmentation could easily be compared to other reports and were found to be in agreement. Considerations had to be made between outputted parameters for a comparison of the location effects. These were also found to be in agreement.

Contents

1 Introduction

1.1 Overview

During this study, surface water flooding has been investigated using two computer models (MacTVD and JFlow) capable of simulating the hydrodynamics involved in rainfall-runoff processes. The effect rewilding, a Natural Flood Management (NFM) method, has on surface water flow has been analysed as it is important to understand how resilience to the upcoming water challenges can effectively be increased. MacTVD has been validated against laboratory data and calibrated for the baseline case. JFlow has been evaluated against this baseline case in MacTVD, as well as against theory, before rewilding patterns were simulated. A comparison between the two models was made and the factors influencing the effectiveness of rewilding have been analysed.

1.2 Context & Significance

Surface water flooding is becoming an increasingly pressing problem due to the increase in frequency and intensification of weather events [Jenkins et al., 2008]. Heavier rainfall is occurring for longer periods of time causing the soil to become saturated more frequently. This means it cannot absorb as much water, resulting in an increased volume of surface water. Flash floods are caused by surface water flow instead of ground water flow as the infiltration process to ground water takes much longer allowing the volume of water to arrive at the outlet at a lower rate over a longer period of time. Therefore this increase in surface water flow, as well as ineffective drainage infrastructure, increases the risk of flash floods. In the UK, 10 000 houses per year are currently being built on flood plains [Allen and Bounds, 2015] and so are at significant risk of surface water flooding. By 2050 the number of people at risk from surface water flooding in a 1 in 200 year storm is predicted to increase by over 50% to 3.2 million [Houston et al., 2011].

Historically flood risk studies have been focused on fluvial and coastal flooding [Douglas et al., 2010]. However it is estimated that 40% of flood damage costs arise from surface water flooding [Harman, 2007]. As a result there has been a policy push to increase the resilience of surface water management systems and to include it in UK design philosophy [Dadson et al., 2017]. The Adaption Sub-Committee of the Committee on Climate Change also called for a more integrated catchment based approach in 2015 [Brown et al., 2017]. An example of this policy shift can be seen in the Autumn Statement in 2016 where £170 million was allocated to increase infrastructure resilience against rising flood risk [McEwan, 2016] of which DEFRA secretary, Andrea Leadson, announced £15 million to be allocated specifically on catchment-scale Natural Flood Management (NFM) measures [Ferguson, 2018]. The progress towards this currently remains at research level and is mainly focused on the improvement of drainage systems [Maho, 2018]. However with the increasing availability of topographic data and advances in computer capabilities, more detailed studies of rainfall-runoff processes can be completed at a catchment scale.

Rewilding, an NFM strategy, has been identified as an appropriate way of increasing resilience against this rising flood risk on a catchment scale. It involves working with natural processes to restore ecosystems and reduce flood risk in the uplands and floodplains [Driver, 2016]. There is increasing evidence and support for this approach, however "it will need political leadership from the highest level to make it happen" (Katherine Pygott, Chartered Institution of Water and Environmental Management, 2014). It has been found that land management practices, in particular the natural regeneration of trees and scrub, can significantly reduce flooding, soil erosion and water pollution [Confor, 2015]. In the Pontbren Project [Wheater et al., 2008], where belts of trees were planted across sheep pastures, an estimated 29% reduction in peak discharge was found for a storm event when only 5% of the upland landscape was reforested. The National Trust [National Trust, 2008] showed that this approach is applicable for 97% of England and Wales. This shows that rewilding could provide a significant reduction in flood risk and could be applied at a national scale. Despite this, there is a lack of implementation of this method due to a number of key factors. For example: there is a lack of information about how to plan and design for optimal land use; and policy barriers such as the Common Agricultural Policy (CAP) requiring land to be kept bare for the basic payment to farmers under Pillar One [Rural Payments Agency, 2015].

1.3 Research Objectives

In response to these upcoming challenges and policy changes, this study focuses on land management practices and in particular on the natural regeneration of trees and scrub to reduce flooding. The general aims of this study are to increase the understanding of rewilding and provide information on how it can be used most effectively to combat the increasing risk of surface water flooding. In order to achieve this the specific aims of this project are to:

- Validate flood modelling software including MacTVD and JFlow against laboratory data and theory.
- Understand the limitations of the software.
- Understand the effectiveness of different rewilding patterns in order to help plan and design for optimal land use.

2 Literature Review

2.1 Rainfall-runoff Processes in Urban Environments

Maho's Masters project [Maho, 2018] looked at modelling surface water run-off in urban environments. The project successfully identified and quantified a number of urban parameters to provide knowledge for the design of flood-resilient urban areas in the future. MacTVD was validated against a series of theoretical cases and laboratory data was obtained to test the model against reality. The dimensionless parameters shown in Equations 1 and 2 were proposed. Please see Appendix B for symbol definitions.

$$Q^* = \frac{Q}{iA} \tag{1}$$

$$t^* = \frac{t\sqrt{Sg}}{A^{0.25}} \tag{2}$$

2.2 Natural Flood Management Measures

Guides from the Scottish Environment Protection Agency (SEPA) [Forbes, 2015] and the Environment Agency (EA) [EA, 2018] were used to identify a number of suitable Natural Flood Management Measures. These were then short-listed using Ferguson's report [Ferguson, 2018] to rewilding, runoff attenuation features, woody debris dams and buffer strips. Ferguson's report, along with further studies [Driver, 2016], shows that rewilding could provide a significant reduction to flood risk and is applicable on the scale required. However there is little information about how to plan and design for optimal use of this NFM scheme. Therefore rewilding has been studied further in this project as its understanding is of great importance for the planning and management of mitigation measures to increase resilience against the upcoming challenges of surface water flooding.

2.3 Impacts of Rewilding

Rewilding changes the land use from bare land or pasture to woodland. This change affects the catchment in the following ways:

- Hydrological parameters. Infiltration rates are increased due to changes in the soil structure and trees intercept water hence reducing the volume of surface water [Yu et al., 2016] [Zope et al., 2017].

- Hydraulic parameters. Increased friction reduces the velocity of surface water and so decreases the rate at which water reaches the rivers. This allows the same volume of surface water to be discharged over a longer period of time and so reduces the peak discharge of a storm event [Ozturk et al., 2013].
- Soil properties. By planting grasslands and woodlands the soil is bound more tightly and so erosion effects are reduced as found in Loess Plateau, China, where cultivated land was turned into grassland and forests [Zhang et al., 2017]. This can also help to reduce the susceptibility to shallow landslides [Persichillo et al., 2017]

In recent years researchers have investigated the effects between land use and rainfall-runoff processes. However most of these studies have been focused on changes to the hydrological parameters due to human activity [Hou et al., 2018]. For example Chaves et al. [Chaves et al., 2008] evaluated the potential of contributing sources for stream flow from pasture and forest in the lowland Amazon region for an entire rain season. Yira et al. [Yira et al., 2016] studied land use changes during urbanisation and established a strong relationship between the reduction of vegetation and the total runoff increase. However all of these studies only investigate the trend between runoff and land use rather than analyse how to plan and design for optimal land use.

2.4 Hydrological and Hydraulic Modelling Techniques

Hydrological models are simplified representations of the land part of the hydrological cycle. They cover the processes which influence that amount of rainfall entering the surface water regime, for example infiltration and runoff rates. These models determine the inputs for the hydraulic models. Hydrological models can be classified in the following ways: physically or empirically based; lumped or distributed; and continuous or event based [Forbes, 2015]. The choice of model depends on the sensitivity of the analysis and the data available. However the 2004 study for Defra [Packman et al., 2004] recommended that when modelling the impacts of land use in rural environments on flood generation the model should be distributed, continuous and at least partially physically based.

In previous studies Siriwardena et al. [Siriwardena et al., 2006] used a simple lumped physical rainfall-runoff model to investigate the effects of natural forest cover reduction on runoff. It was found that using the lumped hydrological model it is often difficult to obtain accurate results. Liu et al. [Liu et al., 2006] applied a distributed physical hydrological model to a catchment in Luxembourg and simulated the storm runoff contributions from different land use types.

Hydraulic models use physical equations to represent the runoff processes governed by fluid flow. They are typically classified by their dimension (either 1D, 2D or coupled) and by whether they are steady or unsteady. 1D models are used to represent in-channel flow and can be used to analyse NFM modifications such as: in-stream structures; riparian/floodplain planting; and river morphology restoration. 2D models give a better representation of floodplain flow and storage and are generally used when incorporating changes in roughness due to land use changes (however they do not consider changes to infiltration). Coupled models are used when both channel and floodplain flow must be represented in detail. In steady modelling it is assumed flow does not vary with time and is applicable where floodplain flow is limited. Unsteady flow allows for changes with time and is required where flood wave propagation, flood storage or attenuation within the system is of interest [Forbes, 2015].

There are two principal uses of hydraulic models:

- To investigate the effects of a physical change within the model area.
- To investigate the changes in flows and phasing resulting from NFM on the wider catchment under scenario testing.

Hydraulic models cannot be used to directly investigate changes in erosion, deposition or changes in infiltration or interception due to vegetation.

Norbury et al. used a coupled 1D/2D hydraulic model to investigate the effects of runoff attenuation features [Norbury et al., 2018]. It was found that ”while NFM can contribute to flood risk alleviation, with multiple socio-environmental benefits, NFM can only be part of a more holistic approach”. In this study a 2D hydraulic model will be applied as used by Hou et al. [Hou et al., 2018] when quantitatively investigating the effect of land use on flood patterns.

2.5 Investigating the ability of Natural Flood Management to improve downstream urban drainage functionality

In 2018 a PhD study investigated four NFM schemes (re-wilding, runoff attenuation features, woody debris dams and buffer strips) and their affect on drainage systems [Ferguson, 2018]. The results for rewilding in this report are shown in Figures 1 and 2. Figure 1 shows that the reduction in peak discharge is linear with the percentage of woodland cover in general, however some combinations of fields are more effective than others. The effectiveness of each field can be found in Figure 2 and it can be seen that the effectiveness of each field appears random. This project aims to find the most effective combinations of fields for an idealised catchment to help understand why certain fields are more effective when rewilded than others.

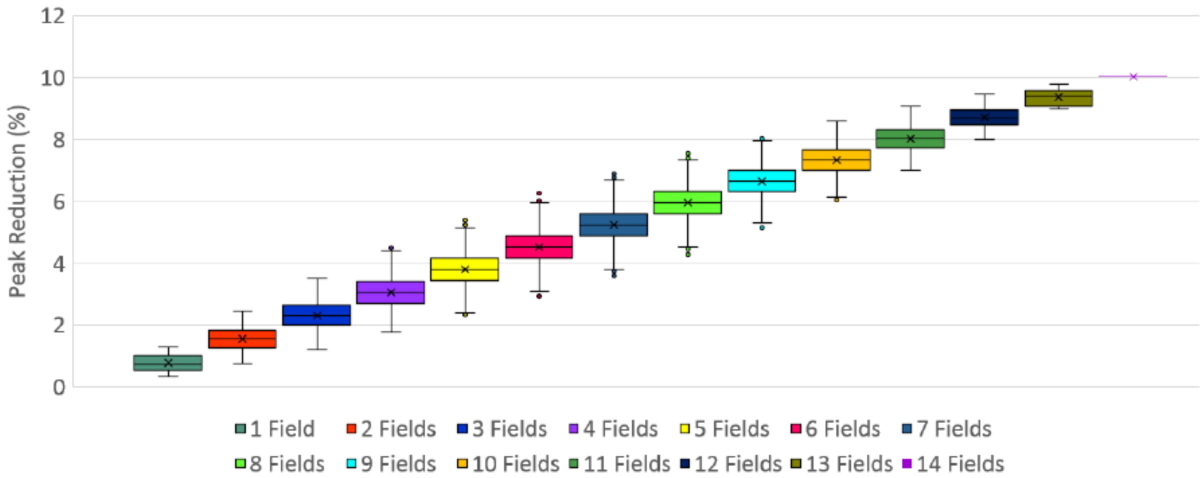

Figure 1: Impact for different combinations of fields on Bin Brook catchment in July 2012 [Ferguson, 2018]

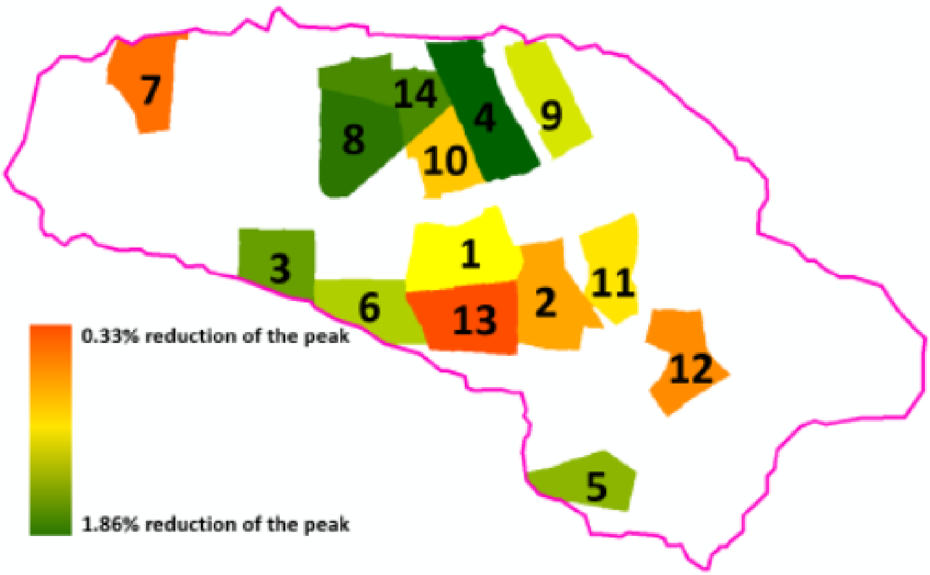

Figure 2: Impact of individual fields on Bin Brook catchment in July 2012 [Ferguson, 2018]

2.6 Assessing Slope Forest Effect on Flood Process Caused by a Short-Duration Storm in a Small Catchment

Hou et al. (2018) quantitatively investigates the effect of land use on flood patterns in an idealised V-shaped catchment for various rainfall events. This report [Hou et al., 2018] concluded the following:

- The effect of the side slope gradient is less sensitive than the channel slope for the same land use and rainfall pattern.
- When the channel slope is less than the critical slope (individual for each catchment),

rewilding the centre of the catchment slope is most effective and rewilding the downstream causes the most servere flooding (maximum peak water levels). Upstream rewilding causes similar peak water levels to central rewilding however the peak discharge is increased.

- When the channel slope is greater than the critical channel slope, rewilding the downstream extent of the catchment is most effective (minimum peak discharge and water levels) while that in the upper and middle have only a slight difference.
- Fragmenting the vegetation has no obvious effect on flood reduction for the same area proportion.
- The flood mitigation extent becomes higher as the rainfall becomes more intense which indicates that optimal land use performs better for heavier rainfall events.

Both the water levels and the peak discharge were used to obtain these findings.

3 Methodology

3.1 Overview

First the computer models (MacTVD and JFlow) were researched to understand the calculations in each and the assumptions they make. Next the software was set up on a personal computer. Previous simulations and experimental data were then reproduced to provide confidence that the input files are being created correctly. Next the model was calibrated for the generic V-shaped catchment shown in Figure 3 which was used as the baseline case for rewilding. The reason for choosing such a baseline case will be explained later in this report. The results of this from each model have been compared to give confidence in the repeatability. The simulations were then run with various re-wilding patterns. The results of these have been collected and analysed.

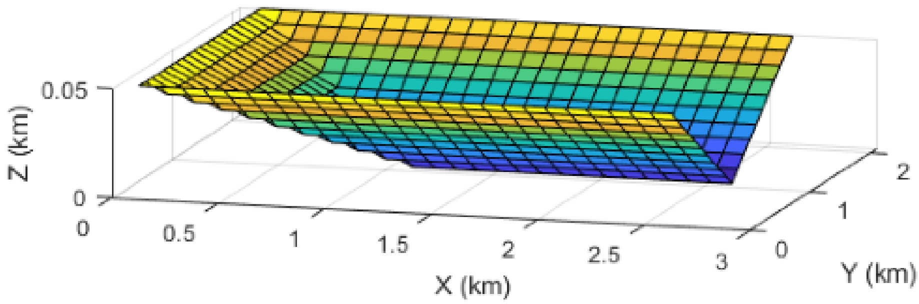

Figure 3: Shape of catchment

3.2 Mathematical Model

With the increasing availability of high resolution topographic data, the two dimensional (2D) shallow water equations (SWEs) have been extensively used and have become the most common model to represent surface water flow [Maho, 2018]. The SWEs are a set of partial differential equations derived from the principles of conservation of mass and momentum in the two horizontal directions. They describe the evolution of an incompressible fluid in response to gravity, bed friction and inertia.

In this study, the depth-averaged dynamic wave approximation has been used. This was shown by Cea et al. to be particularly appropriate for modelling rainfall-runoff processes [Cea et al., 2010]. Additional assumptions include negligible coriolis, wind and viscous forces. A small water depth is also assumed so that vertical momentum exchange can be ignored. Liang et al. defined the general form of the 2D SWEs as described in Equations 3, 4 & 5 [Liang et al., 2006b]. Equation 3 relates to the conservation of mass, Equation 4 the conservation of momentum in the x-direction and Equation 5 the conservation of momentum in the y-direction. These equations are used by MacTVD (please see Appendix B for symbol definitions).

$$\frac{d\eta}{dt} + \frac{dq_x}{dx} + \frac{dq_y}{dy} = 0 \tag{3}$$

$$\frac{dq_x}{dt} + \frac{d(\frac{\beta q_x^2}{H})}{dx} + \frac{d(\frac{\beta q_x q_y}{H})}{dy} = -gH\frac{d\eta}{dx} - \frac{g q_x \sqrt{q_x^2 + q_y^2}}{H^2 C^2} \tag{4}$$

$$\frac{dq_y}{dt} + \frac{d(\frac{\beta q_y^2}{H})}{dy} + \frac{d(\frac{\beta q_y q_x}{H})}{dx} = -gH\frac{d\eta}{dy} - \frac{g q_y \sqrt{q_y^2 + q_x^2}}{H^2 C^2} \tag{5}$$

In this study the Manning roughness value has been used to describe surface roughness. This can be related to the Chézy coefficient used in the SWEs by Equation 6.

$$C = \frac{1}{n} {R_h}^{1/6} \tag{6}$$

JFlow solves the 2D diffusion wave equation, shown in Equation 7, which is obtained by neglecting the acceleration terms in the momentum equations (Equations 4 & 5) [Bradbrook et al., 2004]. This is equivalent to setting the left hand side of the momentum equations equal to zero. The continuity equation is unchanged (Equation 3).

$$\underline{V} = \frac{H^{2/3}}{n} \frac{\nabla(\eta)}{|\nabla(\eta)|^{1/2}} \tag{7}$$

This is appropriate where the flow of water is predominantly driven by the local water surface slope and momentum effects are less significant. Therefore it can only be used for relatively shallow topographically driven flow such as that expected in overland floodplain conveyance [Bradbrook, 2006].

3.3 Numerical Models

This study uses two advanced computer models (MacTVD and JFlow) which are capable of accurately simulating rainfall-runoff processes by solving the 2D equations as described in Section 3.2.

MacTVD solves the SWEs using the Total Variation Diminishing (TVD) MacCormack finite difference numerical scheme. This explicit numerical solution requires careful manual control of the time step to maintain stability. MacTVD also applies a simple shock-capturing model which increases the numerical complexity and therefore the computational cost [Liang et al., 2006a]. Detailed implementation of this scheme as well as numerous validation tests against published experimental data and analytical data have been completed by Liang et al. [Liang et al., 2006b].

JFlow solves the 2D diffusion wave equations using an explicit finite difference scheme. This solves Equation 7 to find the x and y components of velocity using the following equation:

$$\begin{aligned}\nabla(\eta) &= \underline{i}\frac{d\eta}{dx} + \underline{j}\frac{d\eta}{dx} \\ &= \underline{i}\frac{\eta_{\mathrm{i,j}} - \eta_{\mathrm{i+1,j}}}{\Delta x} + \underline{j}\frac{\eta_{\mathrm{i,j}} - \eta_{\mathrm{i,j+1}}}{\Delta y}\end{aligned} \tag{8}$$

A discritised continuity equation is then applied to each grid cell to find the new water depth in that cell. This numerical scheme has an adaptive time step and is conditionally stable based on the Courant-Freidrichs-Lewy (CFL) condition and flow reversal. It is not shock-capturing as the equations cannot represent such hydraulic transients and instead it actively smooths them out [Hunter et al., 2008]. Bates et al. found that diffusion wave treatment out performed 2D finite element approaches because the simplified equations allowed for a much higher density representation of floodplain topography [Bates and de Roo, 2000]. The background to the model development of JFlow and its technical basis can be found in [Bradbrook, 2006]. A version of JFlow was also evaluated against other industry standard 2D hydraulic models for urban flood simulations [Hunter et al., 2008].

Both MacTVD and JFlow have the following assumptions:

- Water depth is much less than any horizontal distances.
- No infiltration losses.
- Once water has left the simulations through the boundaries it cannot re-enter.

3.4 Simulation Parameters

Both MacTVD and JFlow require the input details specific to the catchment. These details include: the topography; rainfall rates; Manning roughness values; initial conditions and boundary conditions.

MacTVD also requires the input of the time step of the calculations. The parameter has a large effect on the time each simulation takes but also the accuracy and stability of the calculations completed. The calculations are only stable provided Courant-Freidrichs-Lewy (CFL) condition (Equation 9) is satisfied [Maho, 2018]. Please see Appendix B for symbol definitions.

$$\Delta t \leq \frac{C_{\mathrm{o}}}{v}\Delta x \tag{9}$$

The Courant number has been taken to be one in this experiment. This limits the movement of fluid particles to only one computational cell per time step. The characteristic wave speed can be approximated for shallow water using Equation 10 [Arthur, 1950].

$$v \approx \sqrt{gH} \tag{10}$$

Therefore as water depth changes with both Manning roughness and rainfall intensity the time step of the calculations must also be adjusted with each of these as well.

3.5 Model Applications

While learning how to use MacTVD, data from previous simulations and from the laboratory was replicated. To do this the topography of the experimental catchment as shown in plan view in Figure 4a was estimated as well as the location of the walls (shown in red). The Manning roughness (0.009 s/m$^{1/3}$) of the catchment and rainfall intensity (317 mm/hr for 45 s) were used from previous years simulations of the experiment.

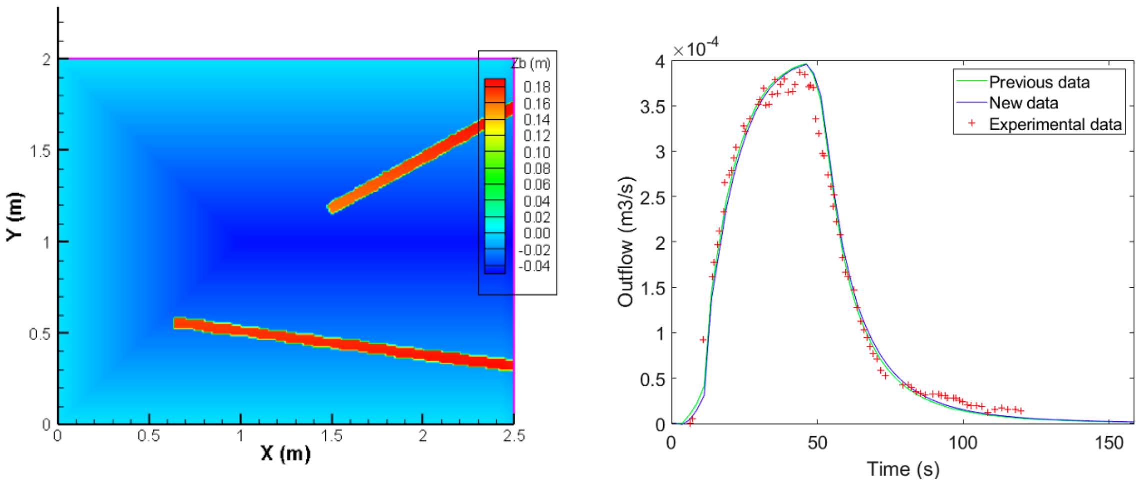

(a) Estimated topography in plan view

(b) Modelled hydrograph compared to experimental data and previous years simulations

Figure 4: Idealised catchment with two walls and uniform rainfall for 45 seconds

Tecplot 360 (a computer graphics program) was then used to visualise and manipulate the data produced. This was done to create the plots in Figure 5 which show how the water depth varies with time over the simulation. The water velocity profiles can be seen in Figure 6. The hydrograph shown in Figure 4b was found by integrating these velocities perpendicular to the catchment edge over the downstream extent. Therefore the water velocity profiles must be checked to provide evidence that the simulations have been completed correctly. This then increases confidence in the accuracy of the hydrographs produced.

The threshold water depths and the time step of the calculations completed by MacTVD were adjusted replicate the experimental data. It can be seen in Figure 4b that the modelled data matches that modelled in previous years as well as the experimental data which increases con-

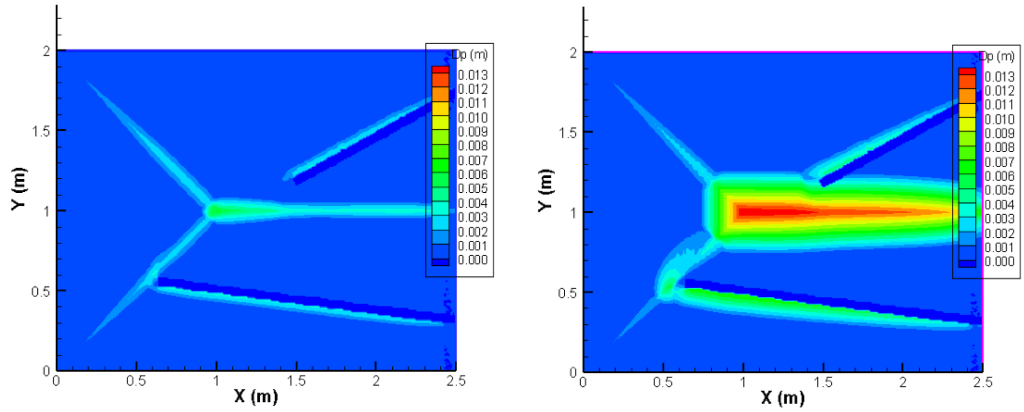

(a) t = 5 s (b) t = 45 s

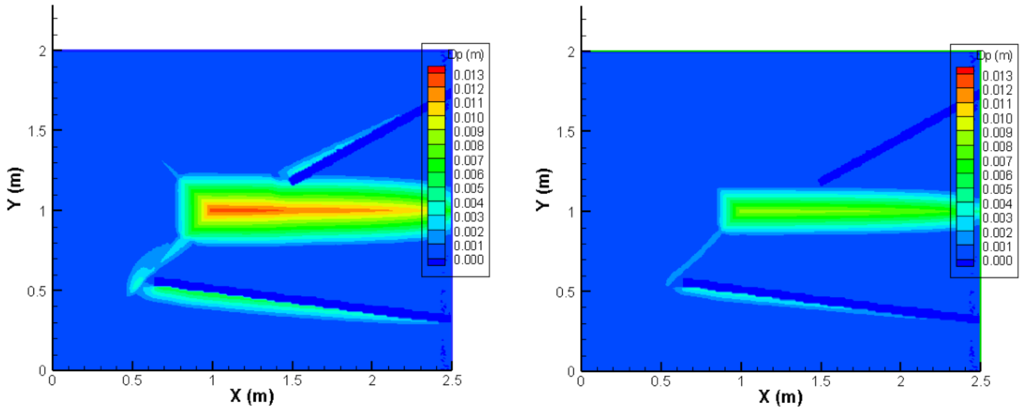

(c) t = 50 s (d) t = 65s

Figure 5: Water depth profiles in plan view

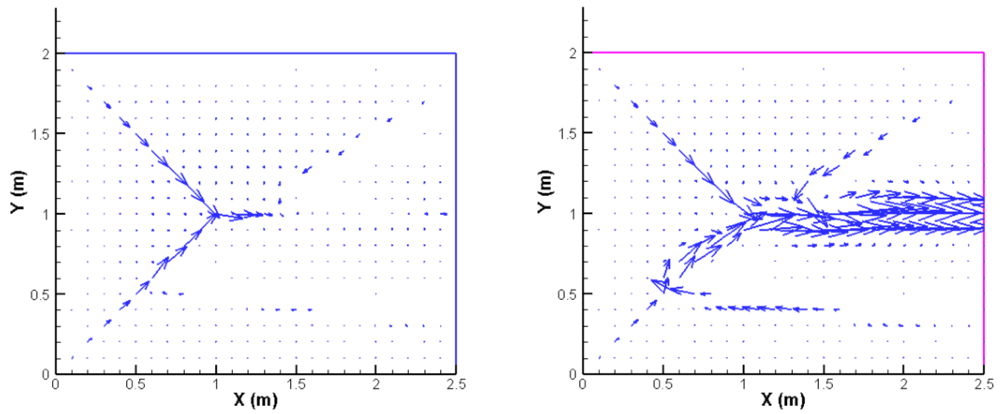

(a) t = 5 s (b) t = 45 s

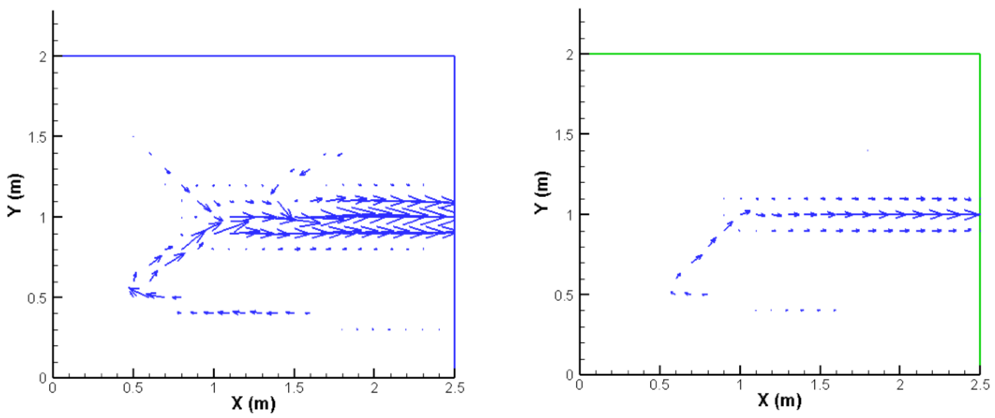

(c) t = 50 s (d) t = 65s

Figure 6: Velocity profiles in plan view

fidence that the input files have been created correctly.

To learn how to use JFlow and associated software (QGIS and PgAdmin) a 3 day course (10^{th} - 12^{th} December) was completed at the JBA Consulting Warrington office. JFlow is unable to accurately simulate a catchment as small as that used to obtain the experimental data. Instead several practice simulations were run before the baseline case completed in MacTVD was set up. A comparison between JFlow and theoretical data will later be made as well as between MacTVD and JFlow for the baseline case.

3.6 Model Calibration

3.6.1 Hydrograph Theory

If a continuous rainfall of constant intensity falls uniformly over an impervious area, the discharge from the catchment will reach an equilibrium at some point. At this point the volumetric outflow rate will equal the volumetric rainfall rate for the catchment. The resulting steady outflow rate will be as shown in Equation 11.

$$Q = iA \tag{11}$$

The time to reach this equilibrium is known as the time of concentration t_c and is the time taken for the water at the furthest part of the catchment to reach the outlet. Work done by Overton & Brakensiek showed that a V-shaped catchment reaches equilibrium according to Equation 12 [Overton and Brakensiek, 1970].

$$t_c = \frac{0.928}{i^{0.4}}\left(\frac{nL}{\sqrt{S}}\right)^{0.6} \tag{12}$$

where: L is defined in feet; and i in inches/hour. Please see Appendix B for all other symbol definitions. The discharge from the catchment can then be calculated at any point using Equations 13 and 14.

$$Q = iA\left(\frac{t}{t_c}\right)^m \qquad for\ 0 \leq t \leq t_c \tag{13}$$

$$Q = iA \qquad for\ t_c \leq t \tag{14}$$

Figure 7 shows the general shape of the hydrograph produced from these equations.

While the time of concentration theoretically characterises the hydrograph response, it is impractical to compare simulated hydrographs this way. As shown in Figure 7 the rate at which

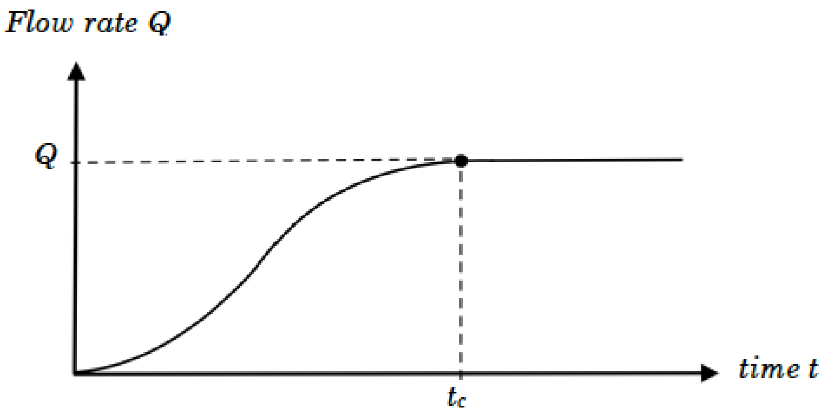

Figure 7: Hydrograph for a catchment under continuous rainfall.

the flow meets steady state is very low due to the S-curve nature of the hydrograph. This means that large errors would occur while estimating the full time of concentration, which is not desired. Instead it is common for researchers to use t_{25} or t_{50}, the times to reach 25% or 50% of equilibrium flow rate respectively. The slope of the hydrograph is much higher here and so the error in the estimation of the time is much less. Lam also showed that having a larger variation in dimensionless time was beneficial for comparing dimensionless hydrographs and recommended that t^*_{70} should be used [Lam, 2016].

3.6.2 Dimensional Analysis

Using the equations in Section 3.6.1 the dimensionless parameters can be derived. From Equation 11 the dimensionless discharge Q* can be found and is shown in Equation 15.

$$Q^* = \frac{Q}{iA} \tag{15}$$

Then using Equation 12 the dimensionless time can be found. This is shown in Equation 16.

$$t^* = t\, i^{0.4} \left(\frac{\sqrt{S}}{nL} \right)^{0.6} \tag{16}$$

It is worth noting that the dimensionless equations are not valid at low roughness values [Overton and Brakensiek, 1970] and instead the results described in Section 2.1 should be used which were derived for frictionless slopes [Maho, 2018]. This can clearly be seen when the dimensionless hydrographs are compared in Figure 8. This means that the hydrographs cannot be compared nondimensionally for low and high roughness values. In these simulations the catchment topography was scaled by 1:1000 of that shown in Figure 3 (2.5 m by 2 m, slope 0.05) as initially used when replicating laboratory data. A continuous rainfall of 100 mm/hr was applied uniformly.

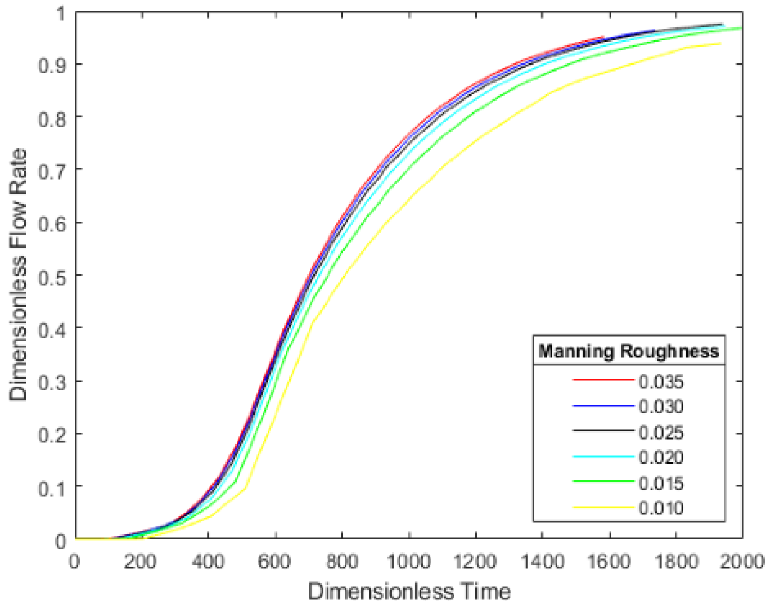

Figure 8: Dimensionless hydrographs for varying roughness in MacTVD

3.6.3 Catchment Scaling

After replicating the experimental data in MacTVD, the catchment was scaled to a more appropriate size for the investigation. The time step was scaled as described in Section 3.4 at each stage and the wetting/drying depths adjusted. The following steps were initially taken:

- Removal of the walls as shown in Figure 4a.
- Application of continuous rainfall.
- Increase in roughness.
- Decrease in rainfall intensity to a realistic value.
- Scaling of catchment size to 2.5 km by 2 km.

After each step the hydrograph was non-dimensionalised according to Equations 15 and 16 in Section 3.6.2. The results were then checked to ensure the simulation parameters had been scaled correctly after the roughness has been increased (hydrographs should converge). However the hydrographs cannot be compared before and after the roughness was increased from 0.009 s/m$^{1/3}$ to 0.035 s/m$^{1/3}$. This is because different equations are required to non-dimensionalise low and high roughness value (as discussed in Section 3.6.2) preventing the hydrographs from converging. The removal of the walls also alter the shape of the hydrograph as does the application of continuous rainfall, however here a comparison can be made initially where the rainfall is unchanged.

3.7 NFM Design

A baseline case was created after scaling the catchment to an appropriate size. The topography of this case is shown in Figure 9. The Manning roughness value used for the catchment was 0.035 s/m$^{1/3}$ and a value of 0.15 s/m$^{1/3}$ was used for any rewilding patterns. These Manning roughness values were chosen using the Environment Agency's Fluvial Design Guide [Crowder, 2009] for short grass and dense brush respectively.

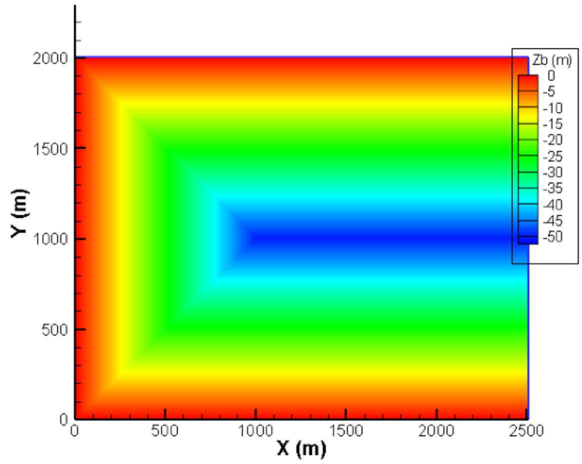

Figure 9: Topography of baseline case for rewilding (m)

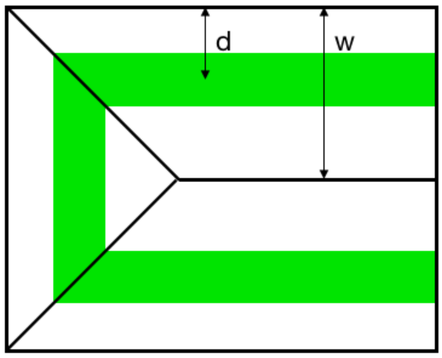

Figure 10: General shape of rewilding band

Various rewilding patterns have then been applied to this baseline case and the increase in time of concentration was measured. The rewilding patterns consisted of bands around the catchment at a certain height (as shown in Figure 10). The width and number of bands have been varied to find relationships relating to location, area coverage and fragmentation of rewilding patterns. When investigating location effects the dimensionless distance $x = d/w$ has been used. For fragmentation, the same dimensionless parameter was used however d is replaced by variable s, the distance between the rewilding bands.

These results were then compared to those found using JFlow. To do this raster files were created using QGIS (a geographic information system application) for the catchment containing the roughness IDs. These IDs were then associated with a Manning roughness value in PgAdmin (a database design and management system). JFlow was then used to complete the computational analysis allowing the outflow to be monitored and water depth grids to be produced. These results were then compared to the results from MacTVD.

4 Model Assessment

4.1 MacTVD Grid Size

Undesirable oscillations were found to occur in the simulated hydrograph data after the rainfall intensity was decreased to 10 mm/hr and the catchment scaled up by a factor of 1000 to the baseline case as described in Section 3.7 (2.5 km by 2 km, slope 0.05, roughness 0.035 s/m$^{1/3}$). These oscillations were thought to be because the width of the deep water channel forming at the bottom of the catchment was narrower than one of the computational grid cells. To combat this the number of grid points used in the input file was increased and the scaling process as described in Section 3.6.3 was repeated. Various grid meshes were trialled and the results can be seen in Figure 11. It can be seen that the smaller the size of the grid cells the smoother the results until the hydrographs converge. However the program took considerably longer to run for more grid points.

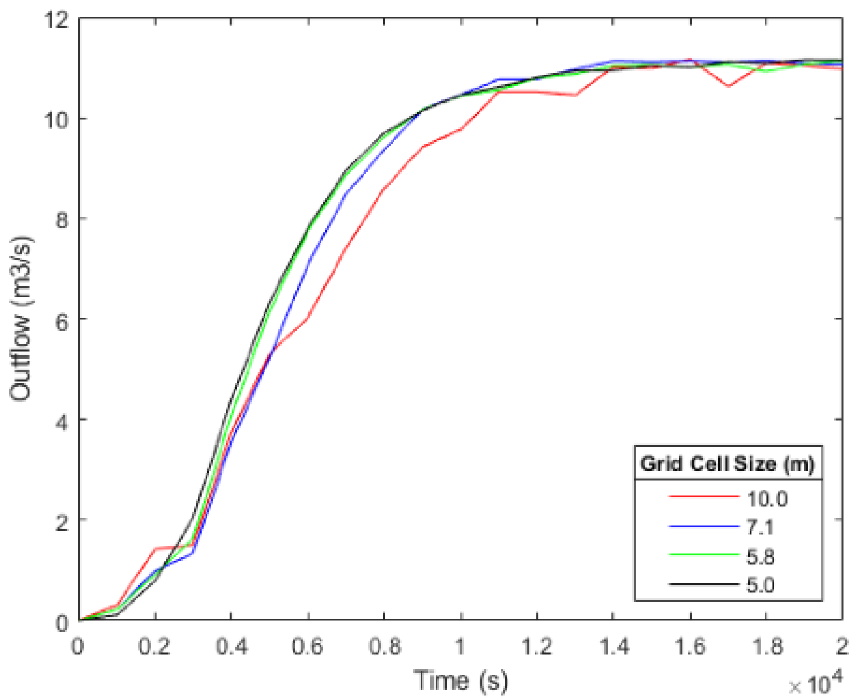

Figure 11: The effect of grid size on the hydrograph for 10 mm/hr of rain.

MacTVD uses a simple shock capturing method which effectively reduces these numerical oscillations and mass balance errors. However as found in Figure 11 these errors are still significant when the grid cell size is not small enough.

4.2 MacTVD at Low Rainfall Intensity

It was noticed there was an error in the equilibrium flow rate for low rainfall intensities while using MacTVD as shown in Figure 12. This error has been quantified in Table 1 and was explored further using the addition of error checking to the fortran code. During this investigation, the simulations were run for the small catchment (2.5 m by 2 m, slope 0.05) to remove any oscillatory behaviour due to grid resolution as discussed in Section 4.1. The rainfall is specified for each result and was applied continuously and uniformly over the catchment. A Manning roughness value of 0.035 s/m$^{1/3}$ was used.

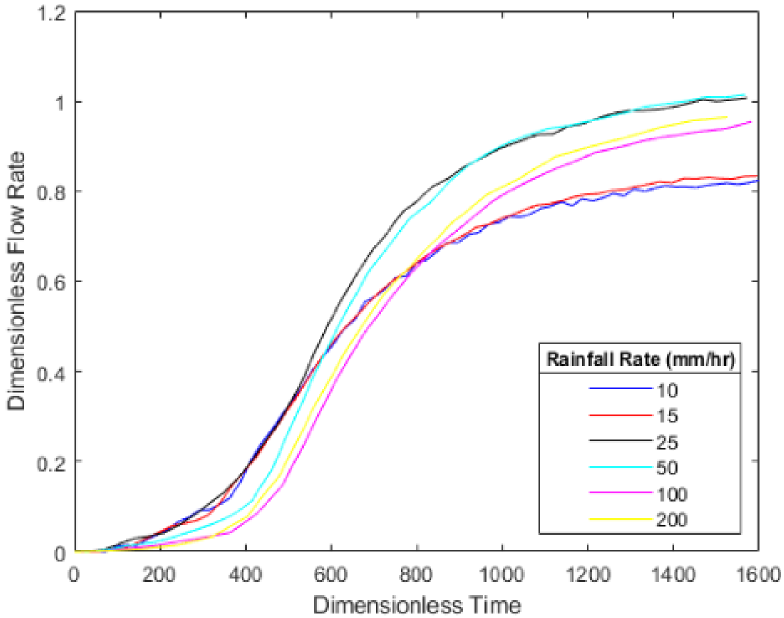

Figure 12: Initial dimensionless hydrographs for decreasing rainfall intensity in MacTVD

It was found that by using a 64 bit double (rather than a 32 bit float) data types for calculations, this error was reduced for lower rainfall rates as shown in Table 1. When compiling the program, the fortran compiler option 'fast' was also used to enable the program to optimise arithmetic operations possible and so run faster.

Figure 13 shows that increasing the precision of the variables has not affected the shape of the hydrographs at high rainfall rates (100 & 200 mm/hr). It has also enabled the hydrographs at rainfall rates of 50 & 25 mm/hr to match more closely with this result as well as reducing the error at equilibrium at lower rainfall rates. However Figure 13 shows that while the hydrographs at low rainfall rates have been improved they still do not converge with the results at higher rainfall rates. It can be seen that at rainfall rates below 50 mm/hr the S-curves start to shift further and further to the left (reaching higher flow rates earlier).

When comparing the velocity profiles for high rainfall intensities and low rainfall intensities, it can be seen that those at low rainfall intensities are not fully developed and have large areas

Table 1: Errors in Equilibrium Flow

Rainfall Rate mm/hr	Calculated Outflow m^3/s	Initial Simulated Outflow m^3/s	Initial Percentage Error %	Improved Simulated Outflow m^3/s	Improved Percentage Error %
360	480	476	-0.9	476	-0.9
180	240	238	-0.7	238	-0.7
50	66.7	65.9	-1.1	66.0	-0.9
20	26.7	26.5	-0.6	26.8	0.4
15	20.0	22.2	10.9	19.8	-1.2
10	13.3	10.8	-18.6	13.2	-1.0
5	6.7	3.2	-52.6	6.6	-1.0

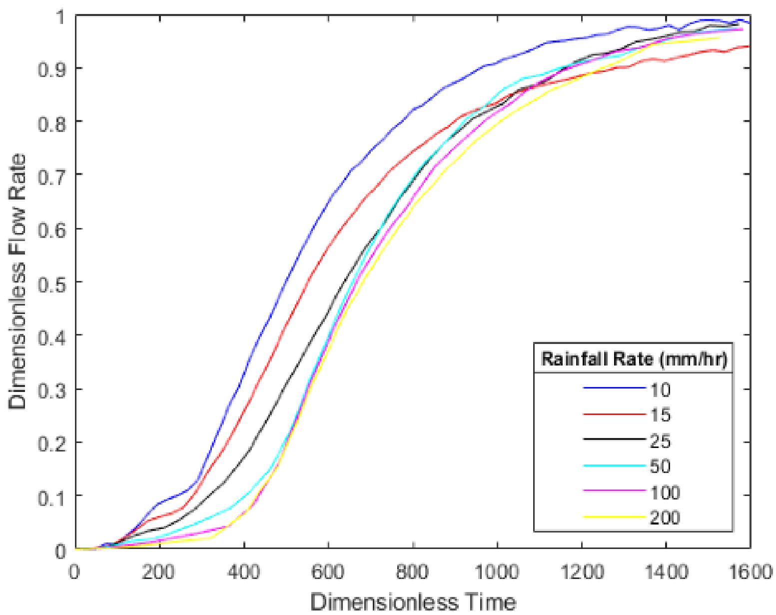

Figure 13: Improved dimensionless hydrographs for decreasing rainfall intensity in MacTVD

with no velocity. On further inspection it can be found that the simulated water depth is zero here as well. This provides evidence that the simulations are not being completed correctly at low rainfall intensities. Figure 14 shows the improvement in the water velocity profiles at 15 mm/hr by increasing the precision of the variables. It can be seen that this improvement has lead to a more developed velocity field, however there is still an area around the channel with no velocity. Figure 15 shows that these areas correspond to areas with zero water depth (note that water depth does not have a linear scale at low water depths to show this more clearly). This provides evidence that while improvements have been made, the problem at low rainfall intensity has not been completely fixed. It is likely that increasing the precision of the variables again would lead to more accurate results.

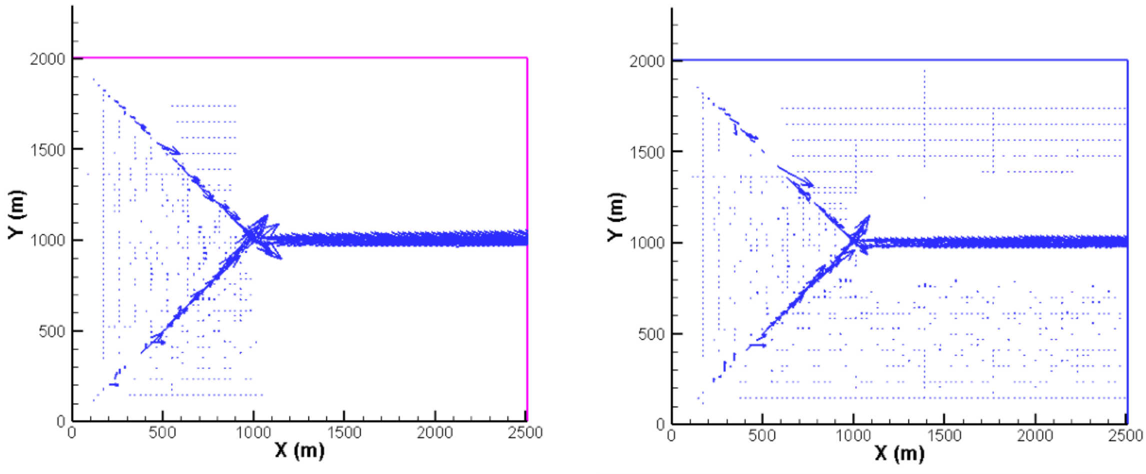

(a) MacTVD

(b) Improved MacTVD

Figure 14: Velocity profiles in plan view at 15 mm/hr rainfall

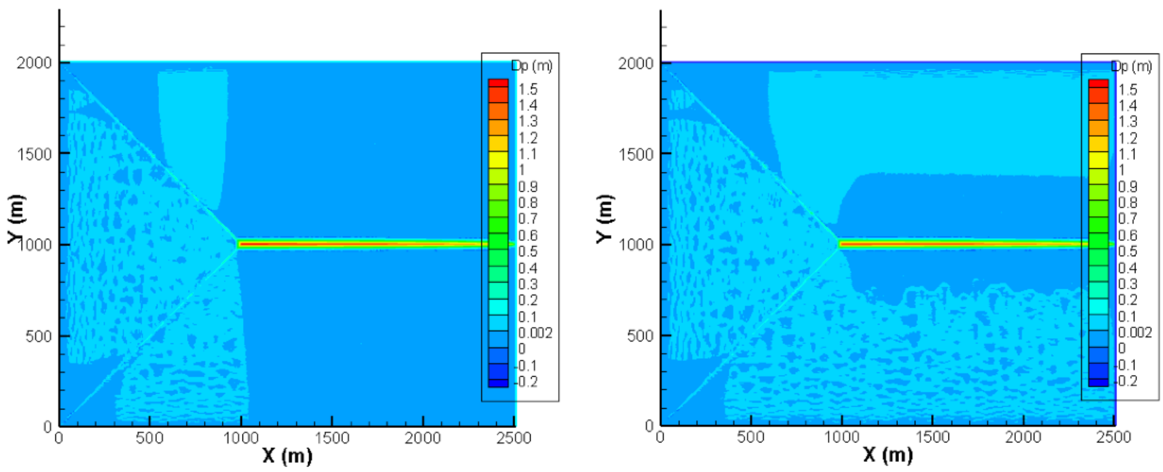

(a) MacTVD

(b) Improved MacTVD

Figure 15: Depth profiles in plan view at 15 mm/hr rainfall

4.3 Comparison between JFlow and Theory

Jflow was initailly tested against the theory in line with the simulations completed by Maho for MacTVD [Maho, 2018]. The catchment is a simple slope of size 800 m by 1000 m and the simulation input parameters can be found in Appendix C Table 5. The results can be seen in Appendix C Figure 33 and are generally unsatisfactory. A version of JFlow was also calibrated against other industry software during the benchmarking evaluation [Hunter et al., 2008].

To obtain more accurate results each of the parameters were changed individually to understand the limitations of JFlow. The results can be seen be seen in Figures 16, 17 and 18. The catchment is the same size as used initially and while each paramater is investigated the others are kept constant at a slope of 0.01, Manning roughness 0.04 s/m$^{1/3}$ and rainfall intensity 100 mm/hr.

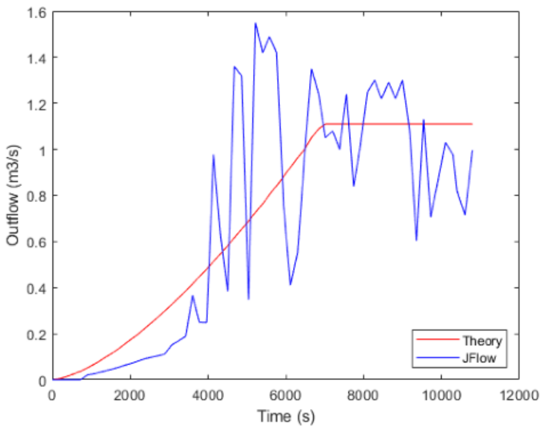

(a) 5 mm/hr rainfall

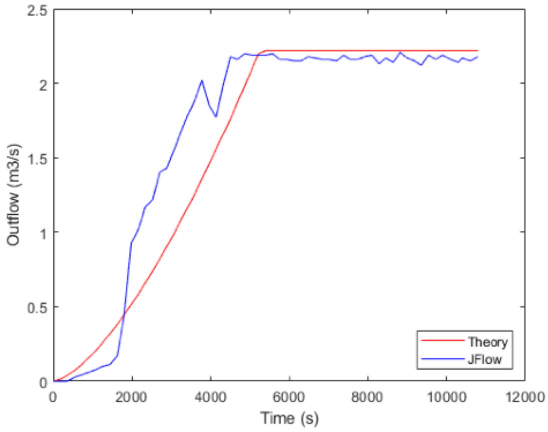

(b) 10 mm/hr rainfall

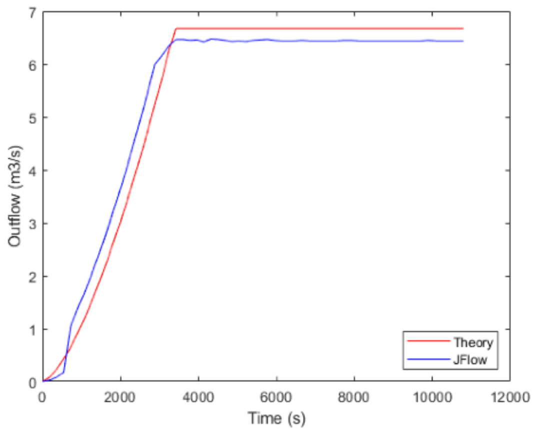

(c) 30 mm/hr rainfall

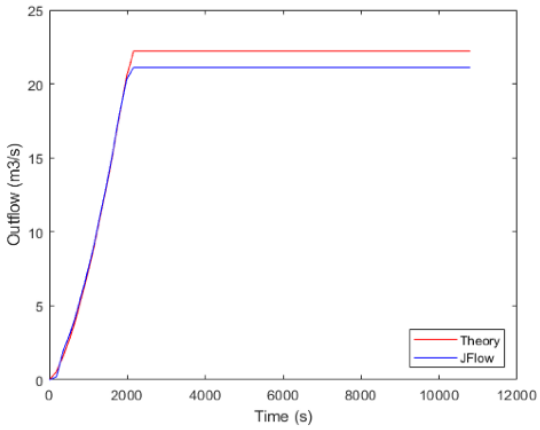

(d) 100 mm/hr rainfall

Figure 16: Simulated hydrographs investigating rainfall intensity

Figure 16 shows that JFlow has problems simulating very low rainfall levels (as also found with MacTVD). The results obtained are of a similar standard to those obtained after the increase of precision in MacTVD. However the results for JFlow are much more obviously wrong and suffer from severe oscillations at low rainfall levels which were not experienced when using MacTVD.

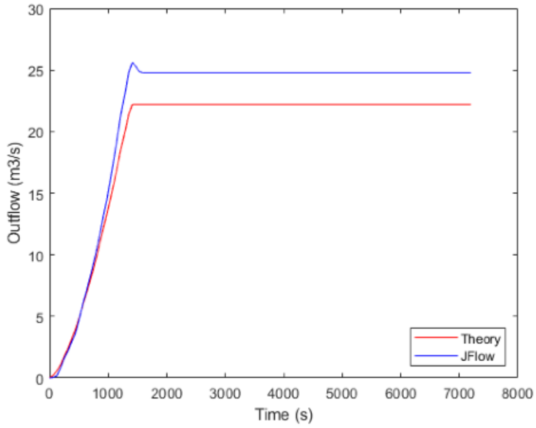

(a) 0.02 s/m$^{1/3}$ Manning roughness

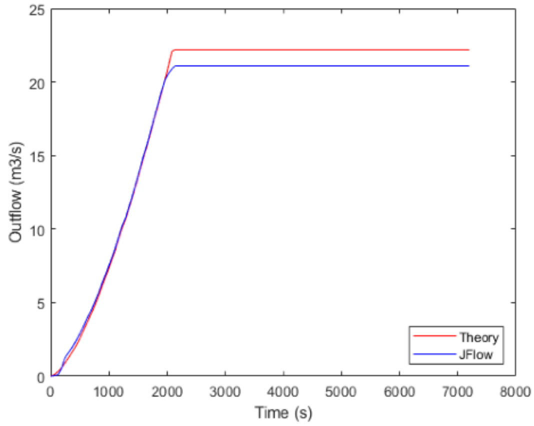

(b) 0.04 s/m$^{1/3}$ Manning roughness

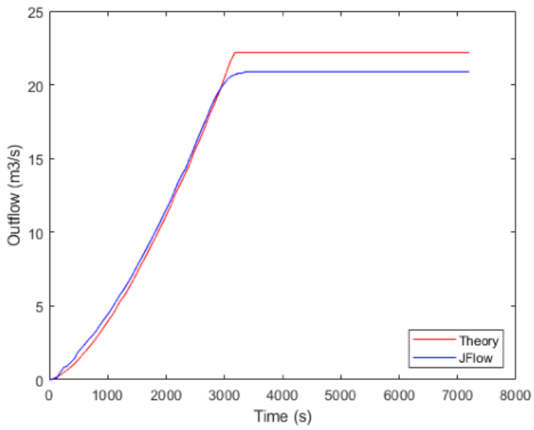

(c) 0.08 s/m$^{1/3}$ Manning roughness

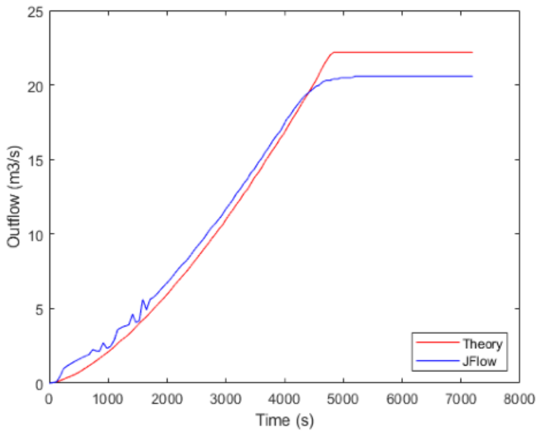

(d) 0.16 s/m$^{1/3}$ Manning roughness

Figure 17: Simulated hydrographs investigating Manning roughness

Figure 17 shows that there is little difference in the accuracy of the simulated hydrographs at higher roughness values. At the extremes there are some slight oscillations which are quickly smoothed out. However there is a significant mass balance error 6% over each case.

As seen in Figure 18 the topographical extremes are simulated poorly by JFlow compared to MacTVD [Maho, 2018]. On considering the mathematical equations solved by JFlow (discussed in Section 3.2) this is unsurprising. JFlow solves the 2D diffusion wave equation which is obtained from the SWEs by neglecting the acceleration terms. This is only appropriate for for relatively shallow topographies where the flow is driven by the local surface slope and momentum effects are minimal.

Undesirable oscillations can also be seen in the results. These were also found in the benchmarking evaluation [Hunter et al., 2008]. JFlow requires an adaptive time step to avoid the development of numerical oscillation and mass balance errors. To do this JFlow implements a

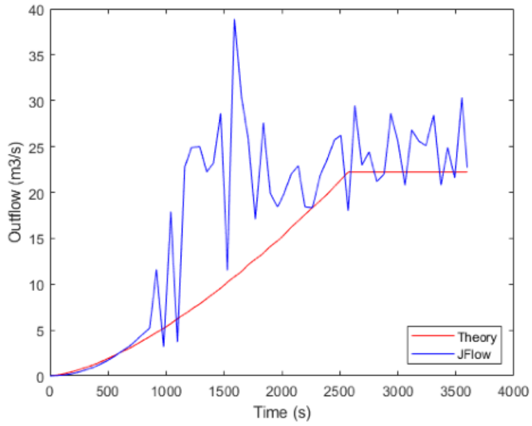

(a) 0.005 catchment slope

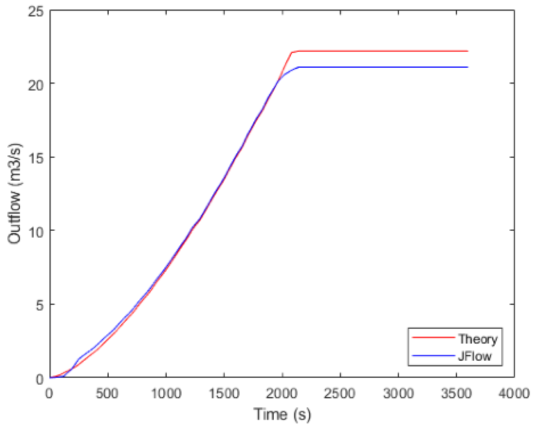

(b) 0.01 catchment slope

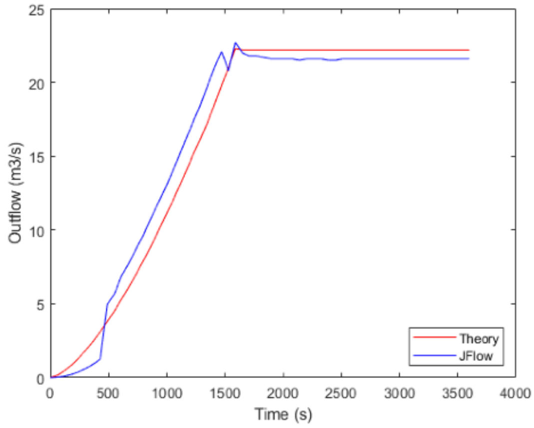

(c) 0.025 catchment slope

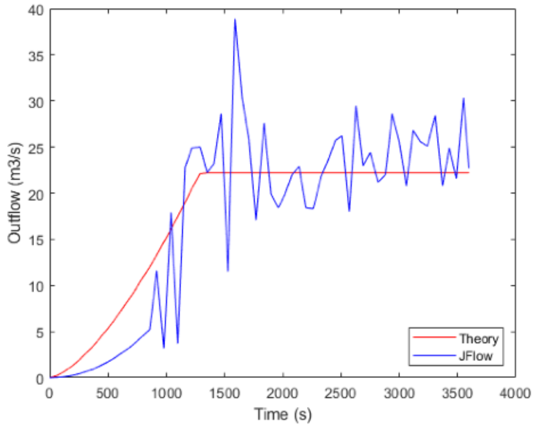

(d) 0.05 catchment slope

Figure 18: Simulated hydrographs investigating catchment slope

conditionally stable scheme based on the CFL condition (see Section 3.4) coupled with a flow reversal constraint. This minimises the potential for oscillations but cannot eliminate them. It was also noted that this oscillatory behaviour was most pronounced at high slope angles, low friction values and low rainfall values. This is because these conditions result in shallower water depths and higher velocities, which enhance oscillatory effects. These oscillations can also be seen in the velocity plots as shown in Figure 19.

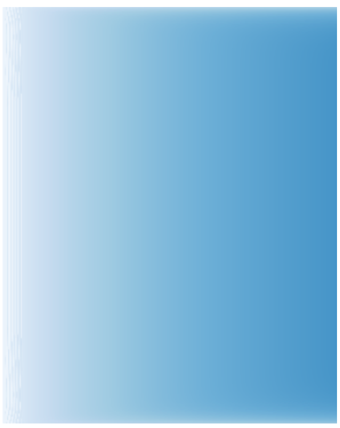

(a) 100 mm/hr rainfall

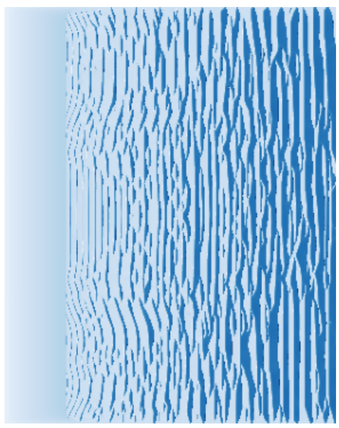

(b) 5 mm/hr rainfall

Figure 19: Velocity plots in plan view

4.4 Comparison between JFlow and MacTVD

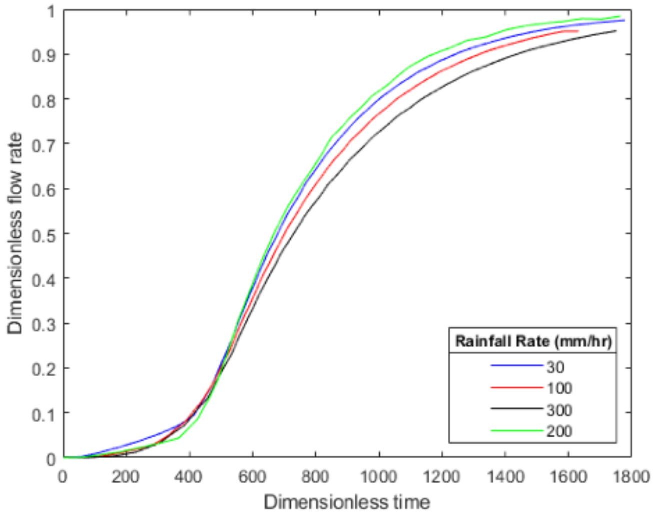

(a) MacTVD at various rainfall intensities

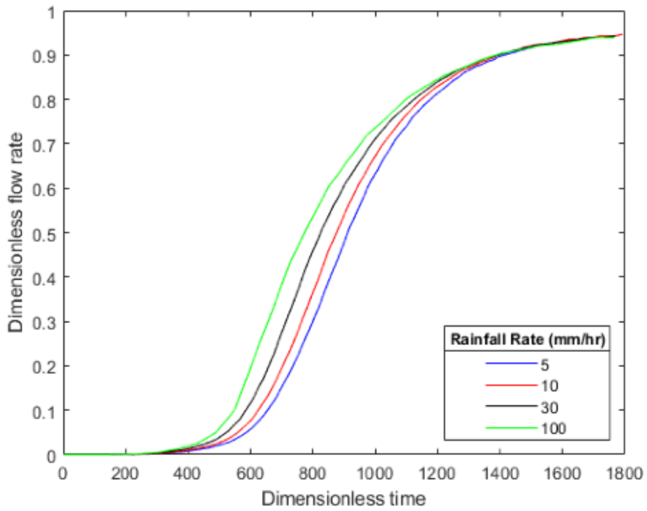

(b) JFlow at various rainfall intensities

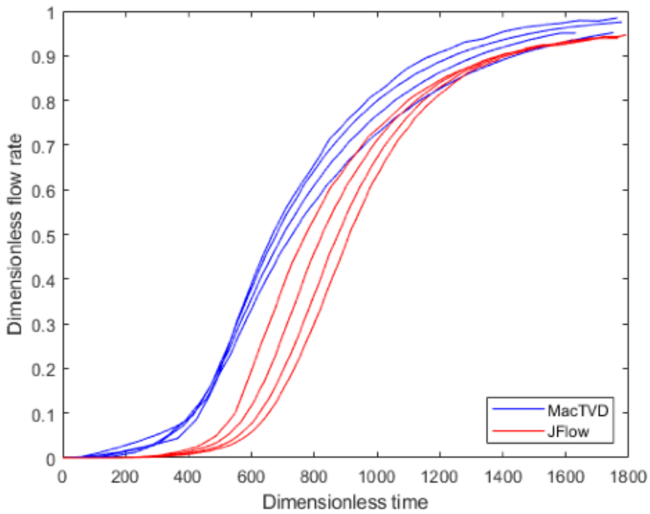

(c) MacTVD compared to JFlow

Figure 20: Dimensionless hydrograph comparison of JFlow and MacTVD

To compare MacTVD and JFlow they have each been run for a variety of rainfall intensities over the same catchment, which will later be used as the baseline case for rewilding. This case has been described previously in Section 3.7 (2.5 km by 2 km, slope 0.05, roughness 0.035 $s/m^{1/3}$). The rainfall has been applied continuously and uniformly over the catchment. The results have been non-dimensionalised and can be seen in Figure 20.

Figure 20a shows that the MacTVD hydrographs converge well with each other, particularly up until t_{50} where they start to diverge slightly. JFlow converges well initially and at peak flow however shows the largest discrepancy at t_{50} as seen in Figure 20b. This diverging behaviour is clearly due to rainfall intensity as t_{50} decreases as rainfall increases.

Figure 20c shows that while the hydrographs are a similar shape, the simulations run by JFlow lag behind those run by MacTVD. Considering the differences between the numerical methods used by both models this is likely to be due to the steepness of the slope preventing the neglection of acceleration terms from being appropriate.

4.5 Implications for NFM Simulations

During the assessment of both models it was found that:

- MacTVD failed to produce accurate data at low rainfall intensities.
- JFlow failed to produce accurate data at high slope angles.
- JFlow uses a spatial raster based approach whereas MacTVD uses text input files.

Due to the difference in the input data files, it was found to be significantly easier and faster to create the NFM pattern inputs accurately for MacTVD than for JFlow. However JFlow would be significantly easier to use if NFM designs were being applied to a real catchment due to its spatial nature. The data collected by MacTVD was also found to converge much better when non-dimensionlised than that collected by JFlow. This means that the data can be compared much more easily and accurately. Overall it was decided that MacTVD should be used to run the NFM simulations and JFlow should only be used to check the results, increasing the reliability of the findings.

Table 2 shows the maximum rainfall intensities measured by the MET Office in the UK [MET Office, 2019]. The sustained rainfall values can be correlated to flood events and would be more preferable for this investigation. Given this data and the length of the simulations to be run this means a rainfall level of 10 to 20 mm/hr would be realistic. However given the problems MacTVD encounters at low rainfall levels the simulations will be completed at higher rainfall levels (100 mm/hr unless otherwise stated) and the dimensionless equations discussed in Section 3.6.2 will be used so the data collected can be applied to real situations. A grid of 433 points by 346 points (cell size 5.8 m) was decided upon as it gave an appropriate trade off between reducing the oscillations in the results and the time taken for each simulation as discussed in Section 4.1. It was also decided that the t_{50} time should be used to compare results as this allows the largest variation and smallest error in estimation (see Section 3.6.1) while ensuring that the results can still be compared accurately when non-dimensionalised (see Section 4.4). This information has been used to create a baseline case which all NFM patterns will be compared to.

Table 2: UK Maximum Rainfall Rates

Duration (minutes)	**Maximum Rainfall Rate (mm/hr)**
5	384
30	160
60	92
120	78
180	59
1440	14

The baseline case has been simulated and the resulting depth and velocity profiles at t_{50} and t_c can be seen in Figure 21. The velocity profiles are fully developed over the whole of the catchment allowing accurate integration to find the hydrograph. This can be seen in Figure 22. The fully rewilded case has also been included to show the maximum possible increase in time to concentration. Figure 22 shows a promising case for rewilding as the time to concentration has been increased by factor 2.3 when the catchment is assumed to be woodland instead of short grass.

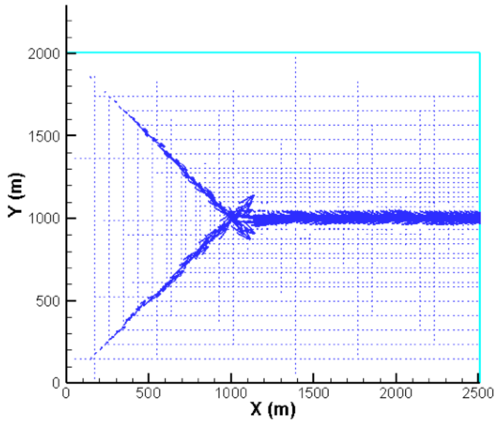

(a) t_{50} velocity profile

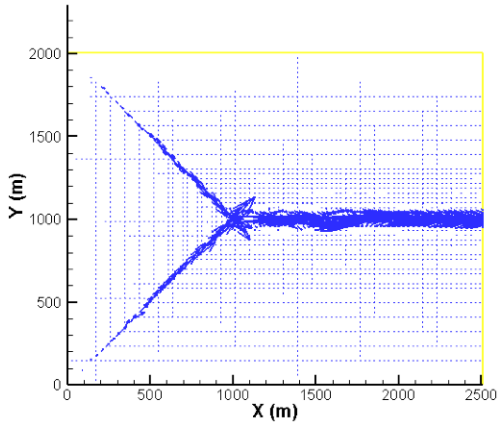

(b) t_c velocity profile

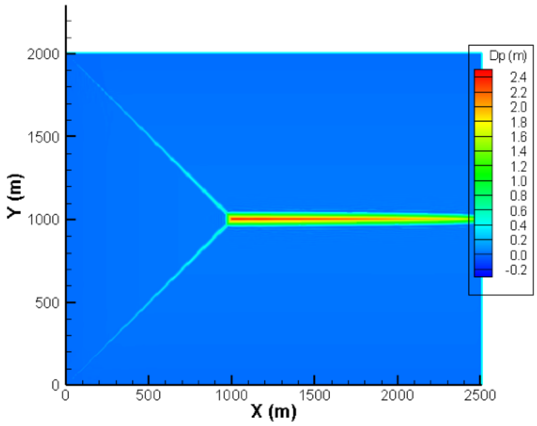

(c) t_{50} depth profile

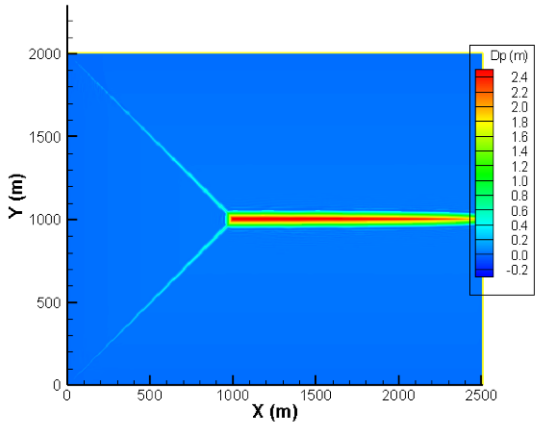

(d) t_c depth profile

Figure 21: Baseline profiles in plan view

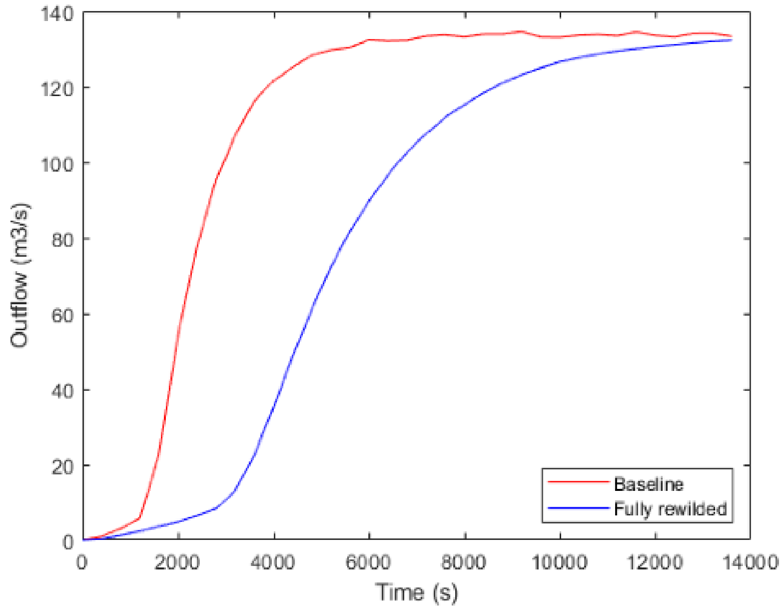

Figure 22: Hydrograph for the baseline case and fully rewilded case.

5 Effects of Rewilding

5.1 Percentage Area

At first the rewilding bands were centred about a line halfway down the slope. Figure 23 shows the water depth plots for 15% and 30% rewilding coverage. It can be seen that the water depth is increased over the rewilding band as the increased friction has slowed the water here. Figure 23b also shows a larger area of increased depth compared to Figure 23a. This implies that a larger volume of water has been slowed down.

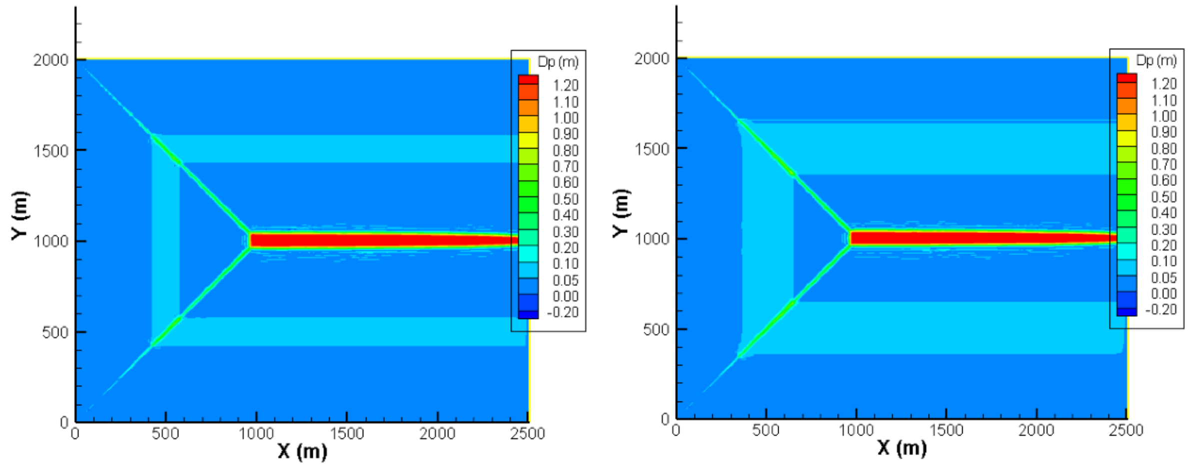

(a) 15% coverage

(b) 30% coverage

Figure 23: Water depth plots for central rewilding

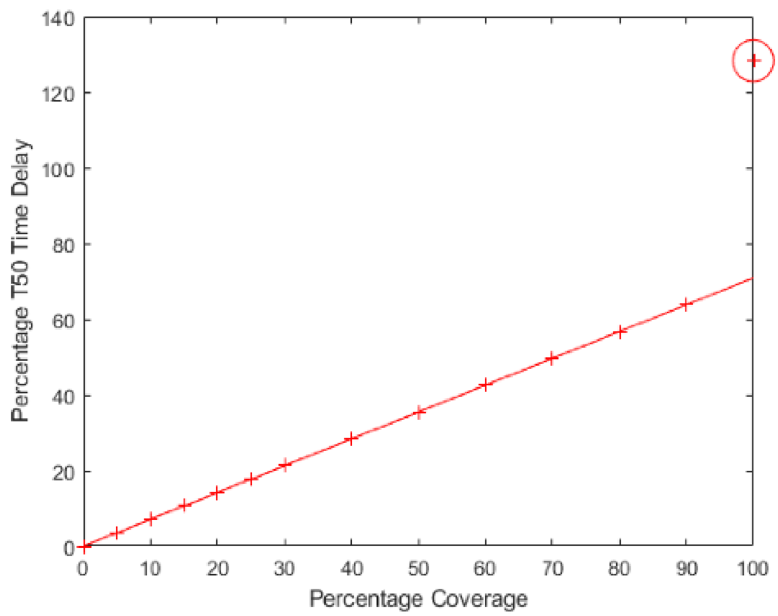

Figure 24: t_{50} time delay for percentage coverage of rewilding band

The time delay at t_{50} compared to the baseline case with no rewilding was measured and can be seen in Figure 24 for various percentage coverage of rewilding. By maintaining a constant central location of the band throughout the simulations, only the size of the rewilding band had an effect on the time delay (there were no location effects). It can be seen that the time delay increases linearly with percentage coverage until almost the whole catchment is rewilded.

When the whole catchment was rewilded it was found that the time delay significantly increased. The simulations were then repeated with the rewilding bands expanding from around the channel and from the top of the slopes of the catchment. The results of these simulations can be seen in Figure 25. This same sharp increase was found within the first few percent of coverage when rewilding around the channel and within the final few percent of coverage when rewilding from the upstream edge of the catchment. This implies there is a location effect associated with the channel which significantly increases the effectiveness of the rewilding.

Figure 25 also shows the time delay increases steeply before levelling off when the rewilding band expands from the channel and increases exponentially when it expands from up-slope. This is different to the linear relationship found in Figure 24 and is because the centre of the rewilding bands location is moving as the width of the band increases. These location effects will be studied in more detail in Section 5.2.

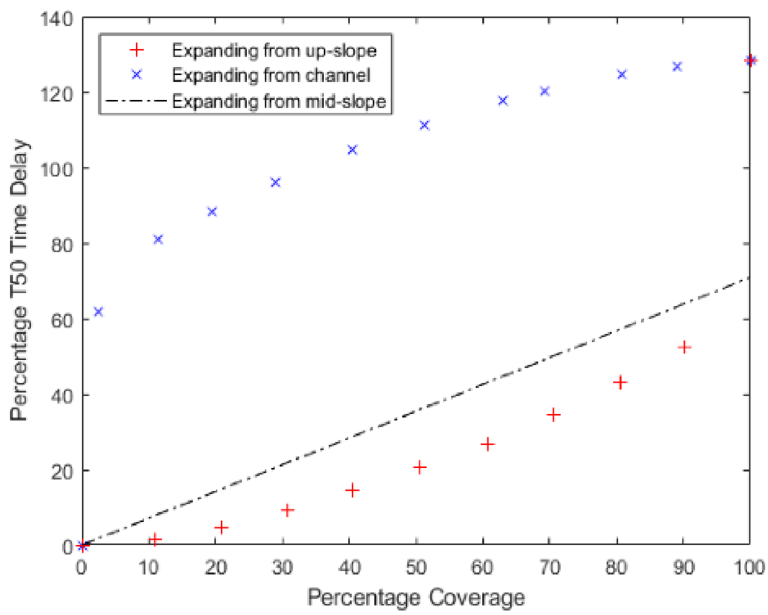

Figure 25: t_{50} time delay for percentage coverage of rewilding band

.

5.2 Location Effects

5.2.1 Rainfall Intensity

The sharp increase in time delay when the rewilding was close to the channel was studied using the small 2.5 x 2 m catchment (all other parameters unchanged). A rewilding band with a constant width of 0.25 m (20% to 30% coverage dependant on location) was moved over the catchment. It was found that different rainfall rates showed this dramatic increase in time delay at different distances from the centre of the channel, as shown in Figure 26. The results were

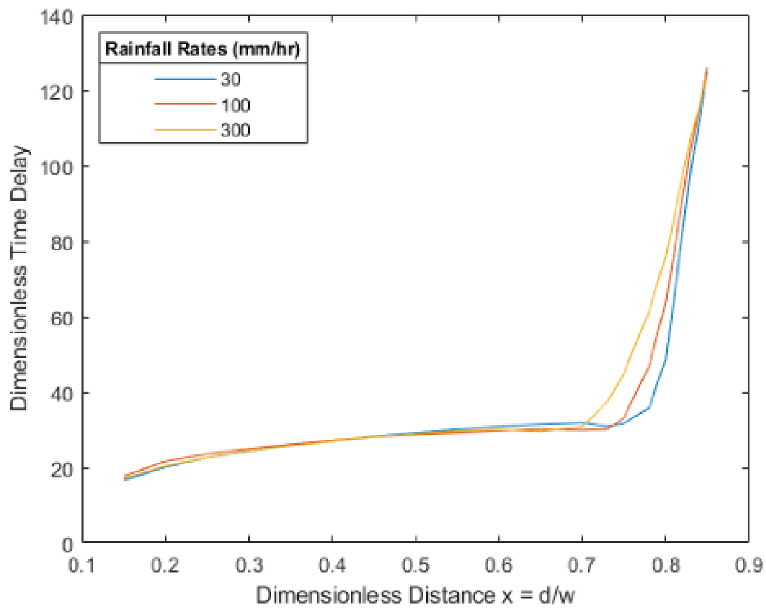

Figure 26: Dimensionless time delay for rewilding bands of constant width

non-dimensionalised to allow the comparison between rainfall rates. The higher the rainfall rate, the smaller the distance from the edge of the catchment before this increase in time delay. It can also be noted that the dimensionless curves converge again after the edge effects of the channel have finished. On further inspection of the water depth plots in plan view (see Figure 27) this difference in dimensionless curves could be because of the increase in water depth or the increase in the width of the channel.

To investigate this further, the profile of the catchment should be changed to a cut rectangular channel rather than a continuation of the V-shaped slopes. This would enable the depth of the channel to be altered with constant width by altering the rainfall rate. The width of the channel could also be altered, however this would likely affect water depths and velocities for a given rainfall rate. There would also likely be problems when trying to simulate this due to the step change in the water surface. Channel flow should also be modelled using a 1D hydraulic model (as mentioned in Section 2.4) and so a coupled model would be best for accurately modelling this interface between the floodplain and the channel.

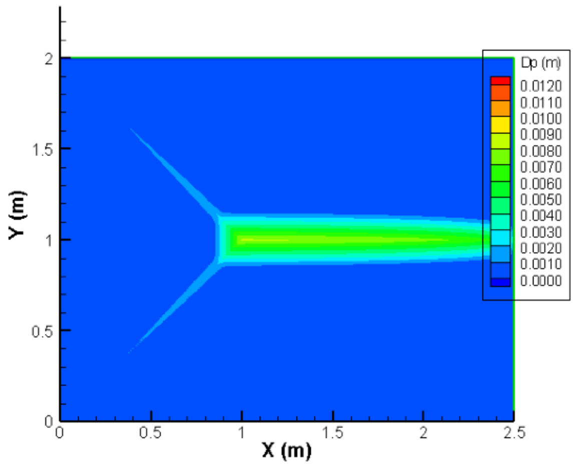

(a) 30 mm/hr rainfall

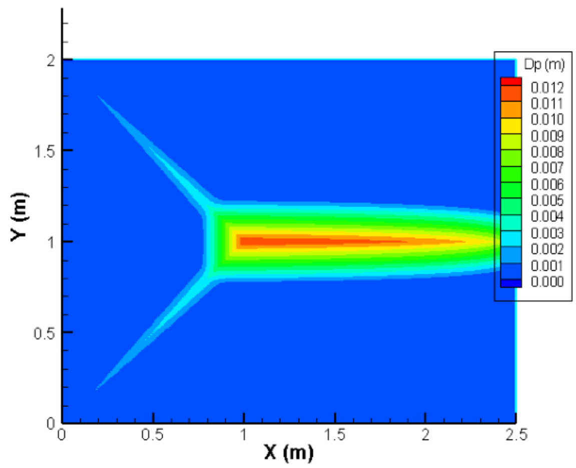

(b) 100 mm/hr rainfall

Figure 27: Plan view of water depth over catchment without rewilding

Another output that should be considered is the maximum water depth at the centre of the channel. The effect of the rewilding location on water depth can be seen in Figure 28. Rewilding the upper and mid slopes has little effect of the depth of the channel compared to the baseline case without any rewilding. However as the rewilding band approaches the already deeper water at the centre of the catchment the maximum water depth significantly increases.

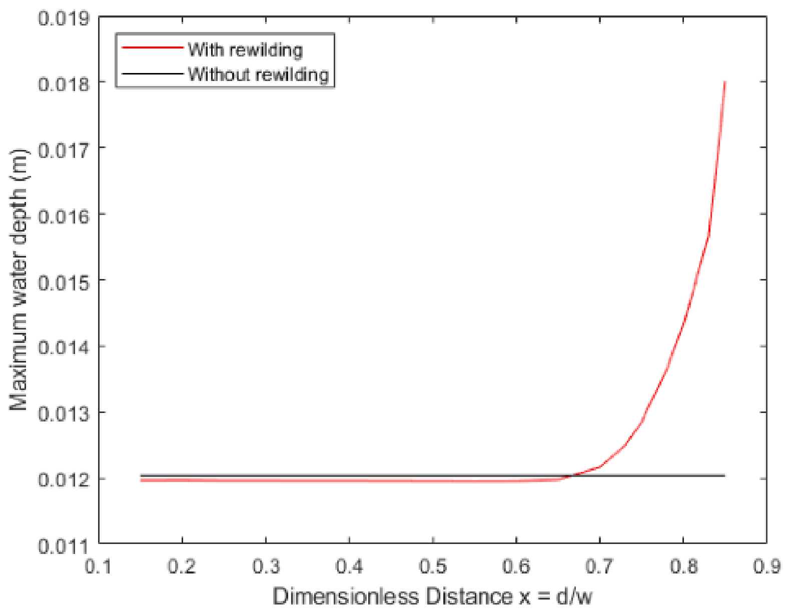

Figure 28: Water depth for rewilding bands of constant width

This means that even though rewilding this central area of the catchment with deeper water is optimal for increasing the time delay (as shown in Figure 26), the water depth is also significantly increased. This may cause more severe flooding local to the rewilding. Therefore it depends on the use of the land and the aim of the rewilding as to whether this is preferable or not. This trade off is also discussed in the work completed by Hou et al. [Hou et al., 2018] on assessing the slope forest effect.

5.2.2 Percentage Coverage

The effect of location was then investigated for the mid and upper slopes of the catchment. The effects were found to be linear with percentage coverage as shown in Figure 29. This means

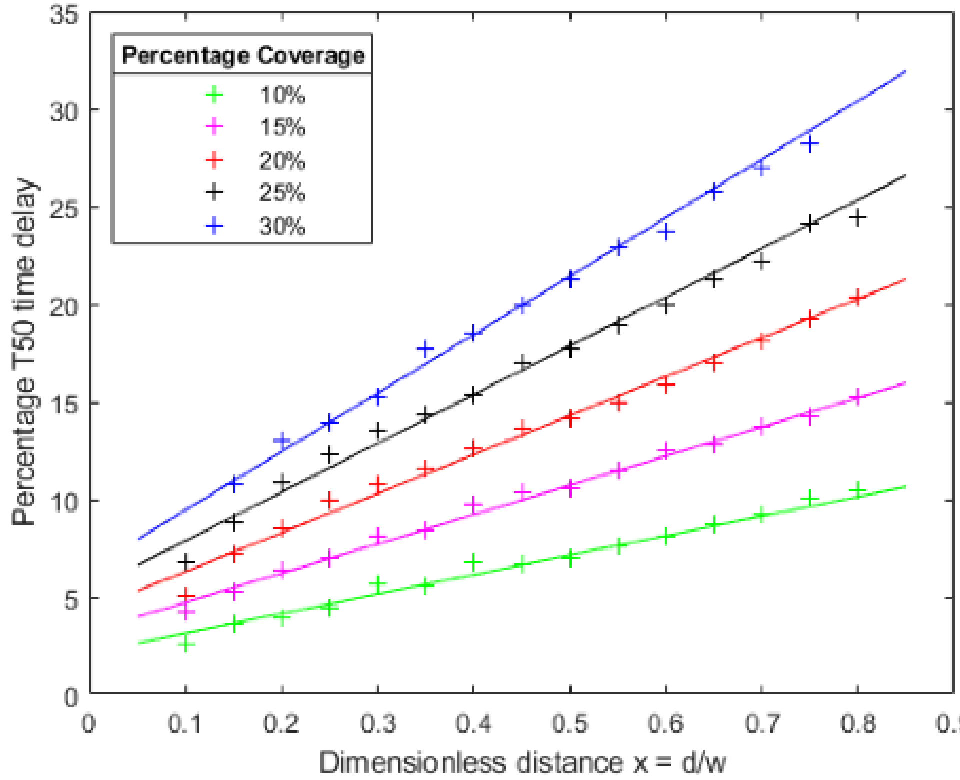

Figure 29: Percentage time delay for rewilding bands of constant percentage width

that the bands must be wider around the channel than at the edge of the catchment. Due to the discrete nature of the model input the percentage coverage could not be kept exactly constant. However the variation was kept within 1% which accounts for some of the slight oscillation around the linear relationship.

Figure 29 shows that not only is the time delay linear with the distance from the edge of the catchment, it is also proportional the the percentage coverage of the rewilding band. This allows a proposed equation to be formed (Please see Appendix B for symbol definitions):

$$\Delta t_p = c_1 p x + c_2 p \tag{17}$$

The values of c_1 and c_2 can be found in Table 3. Using Table 3 an evaluation of these values can also be made. The R^2 value gives an indication of how well the regression line fits that particular set of data with a constant percentage coverage. The standard deviation represents the spread in the values of c_1 and c_2. The R^2 value shows that the regression line for 30% coverage fits the data the best and for 10% the worst.

Table 3: Values of Coefficients

	c_1	c_2	R^2 Value
10%	1.0646	0.1912	0.9858
15%	1.0057	0.2149	0.9935
20%	0.9973	0.2143	0.9897
25%	0.9657	0.2259	0.9913
30%	0.9560	0.2313	0.9965
Mean μ	0.9979	0.2155	
Standard Deviation σ	0.02598	0.4110	

When comparing the standard deviation of both c_1 and c_2 it can be seen that while the standard deviation of c_1 is only 2.6% of the mean, that of c_2 is much higher. It is also noticeable that c_1 decreases as percentage coverage increases while c_2 increases. This effect on c_1 can be accounted for because during the creation of the NFM patterns the actual percentage coverage was slightly above that which was designed for. This effect is largest when the percentage coverage is smallest leading to a slight increase of the values of c_1 and c_2 at low percentage coverage. However this does not explain the discrepancy of c_2.

On considering the predicted data with that collected as shown in Figure 29 it can be concluded that the proposed equation is a good fit. This allows the dimensionless t_{50} time delay to be calculated as follows using the dimensionless equations proposed in Section 3.6.2:

$$\Delta t^*{}_{50} = t^* \frac{\Delta t_{\mathrm{p}}}{100} \tag{18}$$

$$\Delta t^*{}_{50} = t\, i^{0.4} \left(\frac{\sqrt{S}}{nL} \right)^{0.6} \frac{c_1 p x + c_2 p}{100} \tag{19}$$

It is interesting to note that the regression lines converge at the same point when the time delay is zero and the non-dimensional distance is approximately -0.2. At first this was thought to be due to the inside edge of the band reaching the edge of the catchment. However as the bands are different widths the distance from the centre of the band should vary proportionally with the percentage coverage of rewilding rather than remaining constant. This implies there is an edge effect close to the boundary of the catchment which could be investigated further.

5.3 Fragmentation

The effect of leaving a gap between two rewilding bands (each band with constant percentage coverage) was also investigated. This was done by keeping the centre of the two rewilding bands constant at halfway up the slope to remove any location effects. The water depth plots in Figure 30 show that the width of each rewilding band has been altered to keep the percentage of rewilding coverage the same. This has led to a constant area with depth increase. This implies the volume of water slowed by the increased friction is constant and so the time delay compared to the baseline case with no rewilding should be unchanged.

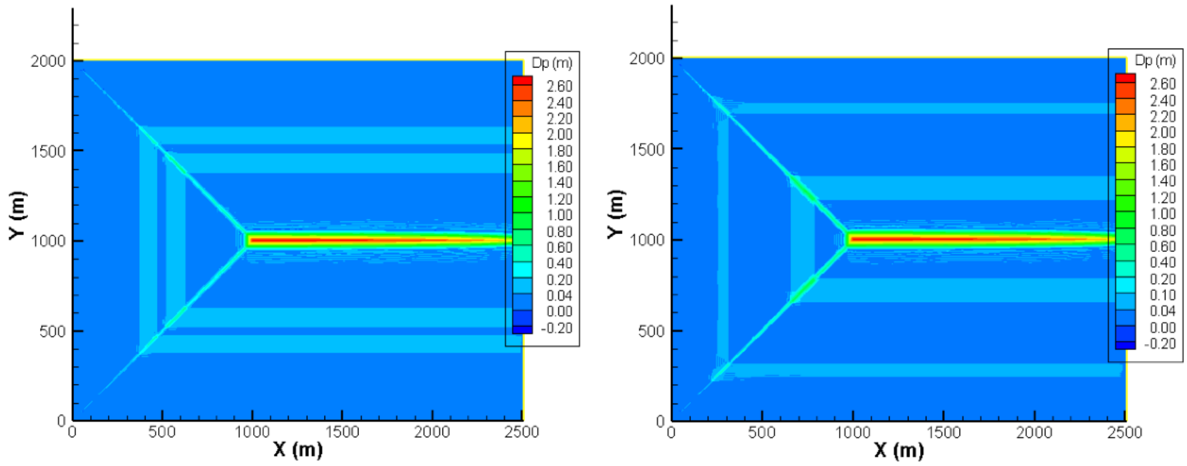

(a) 150 m seperation

(b) 450 m seperation

Figure 30: Water depth plots

The delays at both t_{50} and t_{75} were collected and are shown in Figure 31. It can be seen that there is no consistent correlation between either the fragmentaion and the time delay or the t_{50} and t_{75} results. The spread in the results is ± 0.4% of the average equilibrium time and so the scatter is assumed to be within the tolerance of the model.

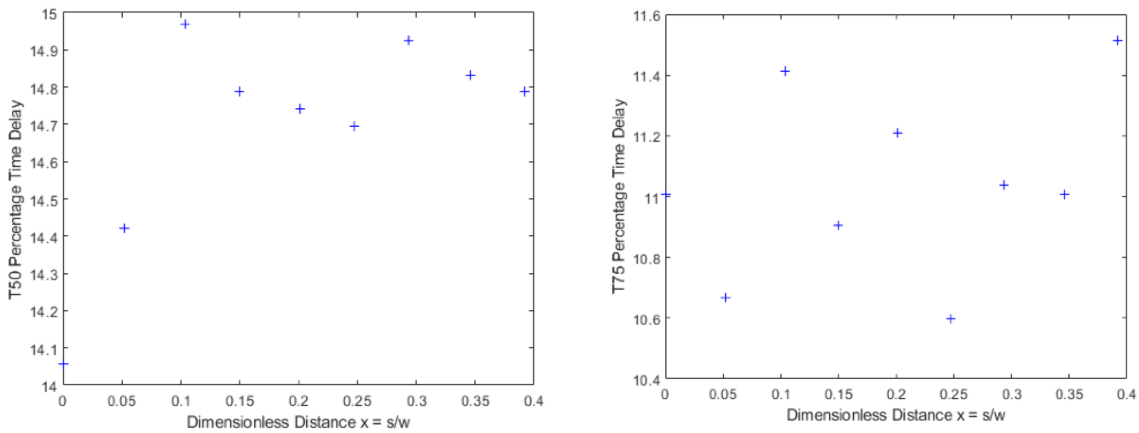

(a) t_{50} time delay

(b) t_{75} time delay

Figure 31: Time delay for fragmentation of rewilding bands with constant percentage coverage

5.4 Comparison with Previous Research

The work completed on the size of rewilding bands centred around the mid point of the slope can be compared to the data collected by Ferguson [Ferguson, 2018] as described in Section 2.5. It can be seen that the linear relationship found in this study (discussed in Section 5.1) agrees with that found by Ferguson.

The data collected in this study on the effects of fragmentation can be compared to the work completed by Hou et al. [Hou et al., 2018]. The conclusions of this previous work have been discussed in Section 2.6. Hou et al. found that fragmentation did not affect affect the flood reduction for a constant area of coverage which agrees with the results of this study discussed in Section 5.3.

However when comparing the findings of Section 5.2 on location effects an easy comparison could not be made. The results described in Section 2.6 for a channel slope of zero imply that the most effective rewilding location for the catchment should be at the centre of the slope [Hou et al., 2018]. This does not agree with the time delays obtained from the simulations from this research. However the research completed by Hou et al. accounted for both the peak discharge from a rainfall event and maximum water levels. In this research the t_{50} time delay for continuous rainfall has been used predominantly. Results from hydrograph time delays and peak discharges should produce concordant results, as an increased time to reach a certain flow rate gives a decreased discharge at a given time (ie. the peak of a flood event).

To make a comparison between this research and that completed by Hou et al. means the water depth profiles for each rewilding pattern must be compared as well. The water depths in plan view can be seen in Figure 32 for the small catchment to highlight the differences in the water depth of the channel. This effect on the central channel can also be seen in Figure 28.

Figure 32 shows that by increasing the roughness you increase the water depth at that location. This effect is most significant when rewilding at the central channel as seen in Figure 32d and starts to occur when the time delay increases steeply as shown when comparing Figure 26 and Figure 28. Figures 32c and 32b show little difference to Figure 32a and so cause no significant increase in water depths. This agrees with the data collected for Figure 28 which shows the maximum water depth in the channel is unaffected by rewilding the upper and mid-slopes.

Using this information as well, it can be decided that rewilding increases the time delay most effectively when used close to the central channel. However water depths rise significantly when the channel itself is rewilded. This gives sufficient evidence that this research agrees with that completed by Hou et al. [Hou et al., 2018].

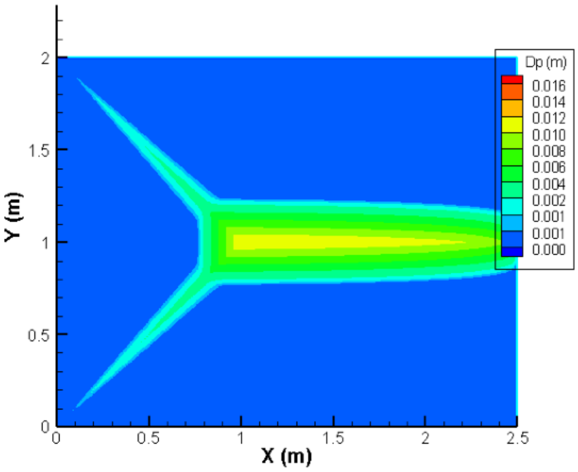

(a) No rewilding

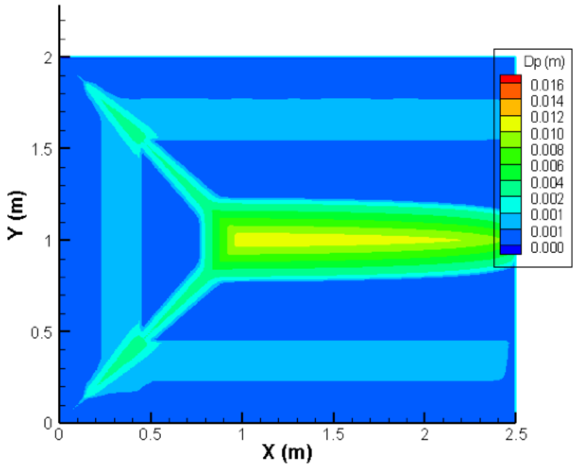

(b) Up-slope rewilding

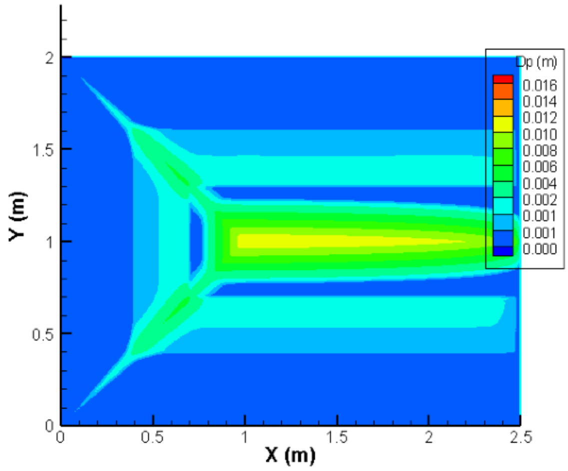

(c) Mid-slope rewilding

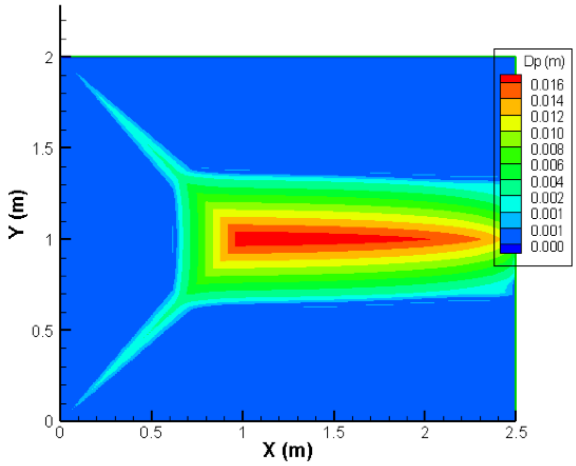

(d) Down-slope rewilding

Figure 32: Plan view of water depths over the catchment for various rewilding schemes.

6 Conclusions

This study set out to increase the understanding of rewilding and provide information on how it should be used to decrease the risk of surface water flooding most effectively. This is particularly important due to the rising flood risk, increased expenditure to cover the damages and policy pushes towards increasing resilience using catchment scale NFM measures. Within rewilding land management practices and specifically the natural regeneration of trees and scrubs have been focussed upon.

Firstly, the flood modelling software had to be validated. MacTVD was compared to laboratory data which had been previously collected. It was found that this experimental data could be accurately replicated by the model. MacTVD has been evaluated against theory in previous years by Maho for larger catchments and found to reliably produce accurate data [Maho, 2018]. JFlow was then used to simulate the same set of theoretical cases as used by Maho for MacTVD.

JFlow was found to perform poorly at high slope angles compared to MacTVD. This is thought to be because of the difference in equations being solved by each model. MacTVD solves the 2D SWEs while JFlow solves the 2D diffusion wave equation which approximates the SWEs by ignoring the acceleration terms. This assumption is only appropriate where the flow of water is predominantly driven by the local water surface and momentum effects are less significant. This is only the case when the topography is relatively shallow. Undesirable oscillations were also found to occur at lower friction values. JFlow requires an adaptive time step to avoid these numerical oscillations and mass balance errors and so implements a conditionally stable scheme based on the CFL condition and a constraint on flow reversal. This minimises the potential for oscillation but cannot eliminate it. The effect is enhanced by shallow water depths and high velocities both of which are caused by low friction values.

A limitation of MacTVD was found while trying to simulate realistic rainfall levels. A significant mass balance error occurred at equilibrium and the dimensionless hydrographs started to diverge at rainfall rates below 100 mm/hr. By increasing the precision of the variables, rainfall rates of down to 25 mm/hr could accurately be simulated and further improvements were made to the error in mass balance errors. It is thought that by increasing the precision further even lower rainfall rates could be simulated accurately. Oscillations could also be found in the results of MacTVD even though a simple shock capturing scheme is applied to reduce these oscillations and mass balance errors. These oscillations were thought to be because the size of the computational grid cells was larger than the width of the deep water channel forming at the bottom of the catchment. They could easily be removed by decreasing the size of the grid cells however this increased the computational cost significantly.

When analysing the effectiveness of rewilding three effects were investigated: area, location and fragmentation. It was found that increasing the area of rewilding led to an increase in t_{50}. The time delay compared to a baseline catchment with no rewilding was found to be directly proportional to the percentage area of coverage if the centre of the rewilding band was kept constant. When the central location of the band changed as the percentage area increased non-linear effects occurred. An increase in water depth over the area rewilded could also be found. However water depths in other areas of the catchment were unaffected.

When rewilding close to the central channel of the catchment a sharp increase in the t_{50} time could be seen. This increase occurred further from the centre when the rainfall intensity was increased and so it thought to be affected by the width of the channel or depth of the water. When the mid and upper slopes (away from the channel) were rewilded a linear relationship between the t_{50} time delay compared to the baseline case and the location of the rewilding could be found. Given the linear relationship between the percentage area of coverage this allowed an equation to be proposed.

Fragmentation of the rewilding was found to have no significant effect which was synonymous with the results from other studies. The data from this study to could be easily compared to Ferguson's work and the results were found to agree [Ferguson, 2018]. However an easy comparison could not be made for the location effects observed. After careful consideration of water depths and the relationship between peak discharge and t_{50} time delay, enough evidence was found to conclude these results agreed with the study completed by Hou et al. [Hou et al., 2018].

Further work in this area of research could include investigating:

- Rewilding close to the channel. A sharp increase in t_{50} time delay was noticed here however a coupled hydraulic model should be used and the 2D models used in this study are not suitable for modelling channel flow.
- Rewilding close to the boundary of the catchment where non-linear effects were noticed. However this area had the least optimal impact on reducing flood risk.
- The effect of different roughness values.
- The effect of different catchment shapes.
- The difference in dimensionless equations found for low and high roughness values.

In conclusion, this study increased the understanding of rewilding and provided information on how it can be used most effectively to combat the increasing risk of surface water flooding. To do this JFlow and MacTVD were validated against theory and experimental data. This enabled the limitations of each model to be evaluated. Various rewilding patterns were then simulated to understand the effectiveness of different rewilding patterns in order to help plan and design for optimal land use.

References

[Allen and Bounds, 2015] Allen, K. and Bounds, A. (2015). Uk building 10000 homes a year on floodplains. Financial Times, News Article.

[Arthur, 1950] Arthur, R. S. (1950). Refraction of shallow water waves: The combined effect of currents and underwater topography. *Transactions, American Geophysical Union*, 31(4):549–552.

[Bates and de Roo, 2000] Bates, P. and de Roo, A. (2000). A simple raster based model for flood inundation simulation. *Journal of Hydrology*, 236(2000):54–77.

[Bradbrook, 2006] Bradbrook, K. (2006). Jflow: a multiscale two-dimensional dynamic flood model. *Water and Environement Journal*, 20(2006):79–86.

[Bradbrook et al., 2004] Bradbrook, K., Lane, S., Waller, S., and Bates, P. (2004). Two dimensional diffusion wave modelling of flood inundation using a simplified channel representation. *International Journal of River Basin Management*, 2(3):211–223.

[Brown et al., 2017] Brown, K., Mauro, M. D., Holmes, G., and Westlake, S. (2017). Progress in preparing for climate change: 2017 report to parliament. Technical report, The Committeee on Climate Change.

[Cea et al., 2010] Cea, L., Garrido, M., and Puertas, J. (2010). Experimental validation of two-dimensional depth-averaged models for forecasting rainfall-runoff from precipitation data in urban areas. *Journal of Hydrology*, 382(1):88–102.

[Chaves et al., 2008] Chaves, J., Neill, C., Germer, S., Neto, S., Krusche, A., and Elsenbeer, H. (2008). Land management impacts on runoff sources in small amazon watersheds. *Hydrological Processes*, 22(12):1766–1775.

[Confor, 2015] Confor (2015). The role of productive woodlands in water management. Technical report, Forest Research.

[Crowder, 2009] Crowder, R. (2009). *Fluvial Design Guide: Chapter 7*. Technical report, Environment Agency.

[Dadson et al., 2017] Dadson, S. J., Hall, J. W., Murgatroyd, A., Acreman, M., Bates, P., and-Joseph Holden, K. B., Holman, I. P., Lane, S. N., Connell, E. O., Reynard, N., and Sear, D. (2017). A restatement of the natural science evidence concerning catchment-based 'natural' flood management in the uk. *Proceedings of The Royal Society*, 473, ISSN:1364–5021.

[Douglas et al., 2010] Douglas, I., Garvin, S., and Lawson, N. (2010). Urban pluvial flooding: A qualitative case study of cause, effect and non-structural mitigation. *Journal of Flood Risk Management*, 3(2):122–125.

[Driver, 2016] Driver, A. (2016). Rewilding and flood risk management. Technical report, Rewilding Britain.

[EA, 2018] EA (2018). *Natural Flood Management Measures: A Practical Guide for Farmers in Calderdale*. Environment Agency.

[Ferguson, 2018] Ferguson, C. (2018). *Investigating the ability of Natural Flood Management to improve downstream urban drainage functionality*. PhD thesis, University of Cambridge.

[Forbes, 2015] Forbes, H. (2015). *Natural Flood Management Handbook*. Scottish Environment Protection Agency.

[Harman, 2007] Harman, J. (2007). Review of 2007 summer floods. Technical report, Environment Agency.

[Hou et al., 2018] Hou, J., Guo, K., Liu, F., Han, H., Liang, Q., Tong, Y., and Li, P. (2018). Assessing slope forest effect on flood process caused by a short-duration storm in a small catchment. *Water*, 10(9):1256.

[Houston et al., 2011] Houston, D., Werritty, A., Bassett, D., Geddes, A., Hoolachan, A., and McMillan, M. (2011). Pluvial (rain-related) flooding in urban areas: the invisible hazard. Technical report, Joseph Rowntree Foundation.

[Hunter et al., 2008] Hunter, N. M., Bates, P. D., Neelz, S., Pender, G., Villanueva, I., Wright, N. G., Liang, D., Falconer, R. A., Lin, B., Waller, S., Crossley, A. J., and Mason, D. C. (2008). Benchmarking 2d hydraullic models for urban flood simulations. *Water Management*, 161(1):13–30.

[Jenkins et al., 2008] Jenkins, G., Perry, M., and Prior, M. (2008). The climate of the united kingdom and recent trends. Technical report, Met Office Hadley Centre, Exeter, UK.

[Lam, 2016] Lam, P. (2016). Rainfall-runoff processes in urban enviroments. Master's thesis, University of Cambridge.

[Liang et al., 2006a] Liang, D., Falconer, R. A., and Lin, B. (2006a). Comparison between tvd-maccormack and adi-type solvers of the shallow water equations. *Advances in Water Resources*, 29:1833–1845.

[Liang et al., 2006b] Liang, D., Lin, B., and Falconer, R. (2006b). Simulation of rapidly varying flow using an efficient tvd-maccormack scheme. *International Journal for Numerical Methods in Fluids*, 53:811–826.

[Liu et al., 2006] Liu, Y., Gebremeskel, S., de Smedt, F., Hoffmann, L., and Pfister, L. (2006). Predicting storm runoff from different land use classes using a geographical information system-based distributed model. *Hydrological Processes*, 20(3):533–548.

[Maho, 2018] Maho, E. (2018). *Rainfall-runoff Processes in Urban Environments*. Master's thesis, University of Cambridge.

[McEwan, 2016] McEwan, G. (2016). Building a better case for natural flood management. Horticulture Week, News Article.

[MET Office, 2019] MET Office (2019). https://www.metoffice.gov.uk/public/weather/climate-extremes/#?tab=climateextremes. Webpage.

[National Trust, 2008] National Trust (2008). Land management and flood risk evidence for the pitt review. Technical report, The National Trust.

[Norbury et al., 2018] Norbury, M., Shaw, D., and Jones, P. (2018). Combining hydraulic modelling with partnership working: towards practical natural flood management. *Proceedings of the Institution of Civil Engineers – Engineering Sustainability*, ISSN:1478–4629.

[Overton and Brakensiek, 1970] Overton, D. and Brakensiek, D. (1970). A kinematic model of surface runoff response. *International Symposium Results of Research on Representative and Experimental Basins, IASH*, 96:100–112.

[Ozturk et al., 2013] Ozturk, M., Copty, N., and Saysel, A. (2013). Modeling the impact of land use change on the hydrology of a rural watershed. *Journal of Hydrology*, 497:97–109.

[Packman et al., 2004] Packman, J. C., Quinn, P. F., Hollis, J. M., and O'Connell, P. E. (2004). Review of impacts of rural land use and management on flood generation: Shortterm improvement to the feh rainfall-runoff model: Technical background. Technical report, Defra and the Environment Agency.

[Persichillo et al., 2017] Persichillo, M., Bordoni, M., and Meisina, C. (2017). The role of land use changes in the distribution of shallow landslides. *Science of the Total Environment*, 574:924–937.

[Rural Payments Agency, 2015] Rural Payments Agency (2015). *The Basic Payment Scheme England*. www.gov.uk.

[Siriwardena et al., 2006] Siriwardena, L., Finlayson, B., and Mcmahon, T. (2006). The impact of land use change on catchment hydrology in large catchments: The comet river, central queensland, australia. *Journal of Hydrology*, 326(4):199–214.

[Wheater et al., 2008] Wheater, H., Reynolds, B., Macintyre, N., Marshall, M., Jackson, B., Francis, O., Chell, J., Frogbrook, Z., and Solloway, I. (2008). Impacts of upland land management on flood risk. Technical report, Flood Risk Management Research Consortium.

[Yira et al., 2016] Yira, Y., Diekkruger, B., Steup, G., and Bossa, A. (2016). Modeling land use change impacts on water resources in a tropical west african catchment (dano, burkina faso). *Journal of Hydrology*, 537:187–199.

[Yu et al., 2016] Yu, M., Li, Q., Liu, X., and Zhang, J. (2016). Quantifying the effect on flood regime of land-use pattern changes via hydrological simulation in the upper huaihe river basin, china. *Natural Hazards*, 84(3):2279–2297.

[Zhang et al., 2017] Zhang, L., Karthikeyan, R., Bai, Z., and Srinivasan, R. (2017). Analysis of streamflow responses to climate variability and land use change in the loess plateau region of china. *Cantena*, 154:1–11.

[Zope et al., 2017] Zope, P., Eldho, T., and Jothiprakash, V. (2017). Hydrological impacts of land use-land cover change and detention basins on urban flood hazard: A case study of poisar river basin, mumbai, india. *Natural Hazards*, 87(3):1267–1283.

A Risk Assessment Retrospective

During the initial risk assessment, the major health risks associated with this project were caused by the prolonged use of computers. These included musculoskeletal problems arising from incorrect posture and eye strain from prolonged eye focusing on computer screens.

An attempt to reduce these risks was made by reducing exposure to computers and increasing physical activity. To do this short, frequent breaks were taken as well as regular physical exercise. These breaks were often taken while waiting for computational simulations to finish. Time was also taken to set up regularly used computer screens, keyboards and chairs to improve posture and reduce eye strain.

In retrospect, these risks were highly pertinent to the tasks and could easily have been overlooked causing serious problems. Therefore, similar caution should be applied when working on future projects where these risks are present.

B Symbol Definitions

Table 4: Symbol Definitions

Symbol	Unit	Definition
β	-	Correction factor for the non-uniform velocity profile
Δt	s	Time step of the simulation
Δt_p	s	Percentage t_{50} time delay
Δt^*_{50}	-	Dimensionless t_{50} time delay
Δx	m	Grid resolution
η	m	Water surface elevation above datum
A	m^2	Area of catchment
C	$m^{1/2}/s$	Chézy coefficient, describing surface roughness
C_o	-	Courant number
c_1	-	Constant found experimentally
c_2	-	Constant found experimentally
d	m	Distance from edge of catchment to centre of rewilding band
g	m^2/s	Gravitational acceleration
H	m	Total water column depth
i	m/s	Rainfall intensity
L	m	Length of the plane of the catchment
m	-	Constant dependant on type of flow, chosen to be 1.5 (corresponding to turbulent flow) for this study.
n	$s/m^{1/3}$	Manning roughness value
Q	m^3/s	Volumetric flow rate
Q*	-	Dimensionless volumetric flow rate
p	-	Percentage area of catchment covered by rewilding
q_x	m^2/s	Unit width volumetric flow rate in x direction
q_y	m^2/s	Unit width volumetric flow rate in y direction
s	m	Distance between rewilding bands
t	s	Time
t*	-	Dimensionless time
t_{25}	s	Time to reach 25% of equilibrium flow rate
t_{50}	s	Time to reach 50% of equilibrium flow rate
t_{75}	s	Time to reach 75% of equilibrium flow rate
t_c	s	Time of concentration
v	m/s	Characteristic wave speed
w	m	Distance from edge of catchment to the channel
x	-	Dimensionless distance equal to d/w

C JFlow Simulations

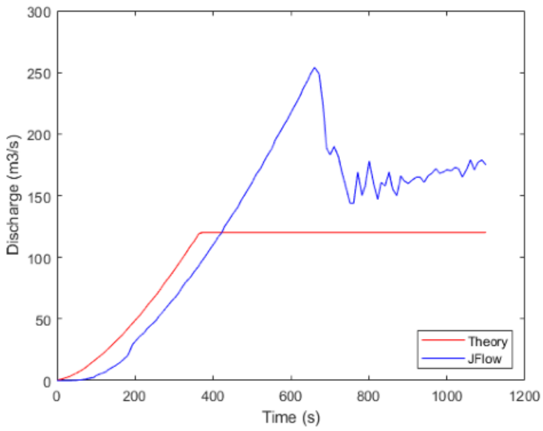

(a) Simulation 1

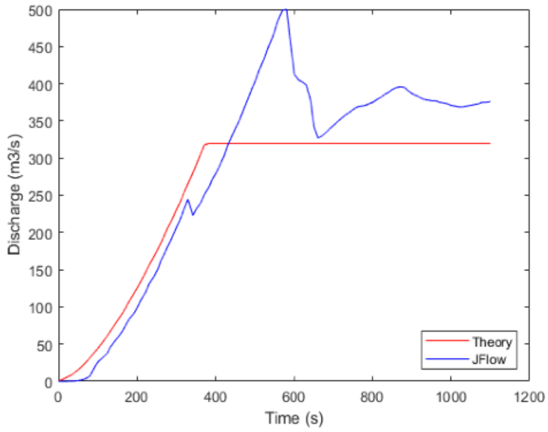

(b) Simulation 2

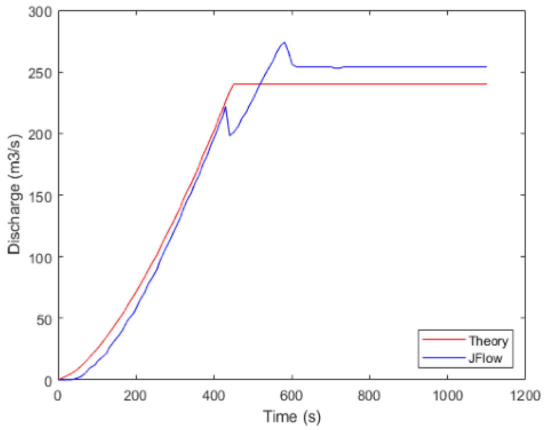

(c) Simulation 3

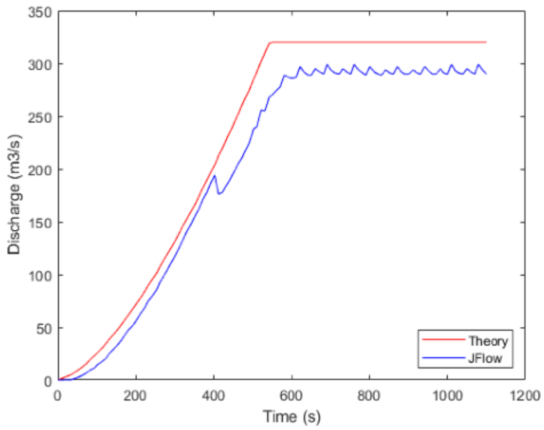

(d) Simulation 4

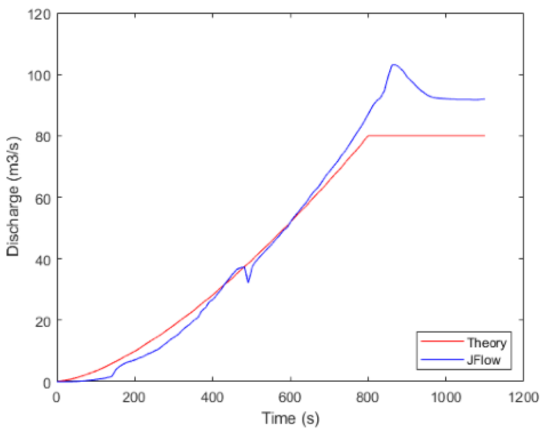

(e) Simulation 5

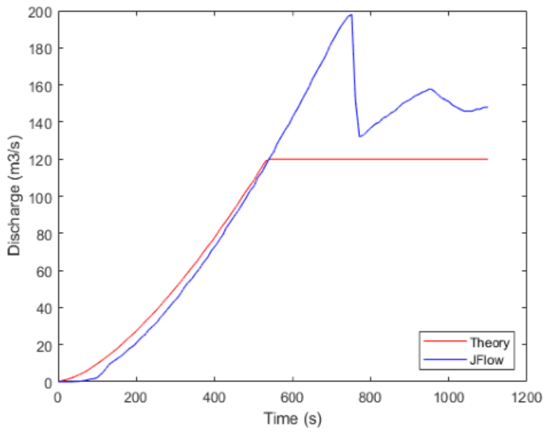

(f) Simulation 6

Figure 33: Simulated hydrographs

Table 5: Simulation Parameters

Simulation Number	**Rainfall Rate (mm/hr**	**Catchment Slope**	**Manning Roughness ($s/m^{1/3}$)**
1	540	0.05	0.015
2	1440	0.05	0.03
3	1080	0.01	0.015
4	1440	0.01	0.025
5	360	0.025	0.03
6	540	0.025	0.02